1

2

3

4

5

6

7   **Recent genetic drift in the co-diversified gut bacterial symbionts of laboratory mice**

8

9

10   Daniel D. Sprockett[1], Brian A. Dillard[1], Abigail A. Landers[1], Jon G. Sanders[1], Andrew H.

11   Moeller[1,2,*]

12

13   [1]Department of Ecology and Evolutionary Biology, Cornell University, Ithaca, NY 14853, USA

14   [2]Department of Ecology and Evolutionary Biology, Princeton University, Princeton, NJ 08540,

15   USA

16   *To whom correspondence should be addressed: andrew.moeller@princeton.edu

17

18

19

20 **Laboratory mice (*Mus musculus domesticus*) harbor gut bacterial strains that are distinct**

21 **from those of wild mice[1] but whose evolutionary histories are poorly understood.**

22 **Understanding the divergence of laboratory-mouse gut microbiota (LGM) from wild-**

23 **mouse gut microbiota (WGM) is critical, because LGM and WGM have been previously**

24 **shown to differentially affect mouse immune-cell proliferation[2,3], infection resistance[4],**

25 **cancer progression[2], and ability to model drug outcomes for humans[5]. Here, we show that**

26 **laboratory mice have retained gut bacterial symbiont lineages that diversified in parallel**

27 **(co-diversified) with rodent species for > 25 million years, but that LGM strains of these**

28 **ancestral symbionts have experienced accelerated accumulation of genetic load during the**

29 **past ~ 120 years of captivity. Compared to closely related WGM strains, co-diversified**

30 **LGM strains displayed significantly faster genome-wide rates of fixation of**

31 **nonsynonymous mutations, indicating elevated genetic drift, a difference that was absent in**

32 **non-co-diversified symbiont clades. Competition experiments in germ-free mice further**

33 **indicated that LGM strains within co-diversified clades displayed significantly reduced**

34 **fitness *in vivo* compared to WGM relatives to an extent not observed within non-co-**

35 **diversified clades. Thus, stochastic processes (*e.g.*, bottlenecks), not natural selection in the**

36 **laboratory, have been the predominant evolutionary forces underlying divergence of co-**

37 **diversified symbiont strains between laboratory and wild house mice. Our results show**

38 **that gut bacterial lineages conserved in diverse rodent species have acquired novel**

39 **mutational burdens in laboratory mice, providing an evolutionary rationale for restoring**

40 **laboratory mice with wild gut bacterial strain diversity.**

41

42

Main Text

Mammalian lineages share gut bacterial taxa (*e.g.*, genera), but bacterial strains within these taxa differ systematically among host populations and species[6–12]. For example, common laboratory lines of house mice (*Mus musculus domesticus*) (*e.g.*, C57BL/6J), which were derived from wild mice > 100 years ago[13], harbor gut-microbiota strains distinct from those of the same taxa found within wild house mice[1]. The evolutionary histories of laboratory mouse–gut microbiota (LGM) strains remain unclear. LGM strains may have been acquired in captivity from external sources, such as humans or the indoor environment. Alternatively, LGM strains may be descendants of ancestral symbionts from the wild-mouse gut microbiota (WGM) that have been reshaped by laboratory-specific evolutionary forces, such as natural selection or genetic drift.

In principle, LGM strains descended from symbioses ancestral to laboratory and wild mice could be identified through co-phylogenetic analyses, which test for parallel diversification (co-diversification) between symbionts and hosts. Discovering ancestral, co-diversifying symbionts in the gut-microbiota (GM) would also provide a phylogenetic framework for interrogation of the histories of symbiont adaptation and genetic drift within host lineages, as has been possible in simpler host-microbe symbioses, such as those between insects and bacterial endosymbionts[14,15]. However, co-phylogenetic tests have not been feasible for rodent gut microbiota due to the limited phylogenetic information provided by 16S rDNA sequencing and assembly-free shotgun metagenomics[16]. Analyses of high-quality bacterial genomes assembled directly from metagenomes[17,18] provide increased power to test for co-diversification between gut microbiota and hosts. These approaches have recently revealed that multiple GM strains have co-diversified with humans and other primate species[8,10] but have yet to be leveraged to assess

65   the evolutionary histories of mouse GM strains, owing to a lack of genome-resolved datasets

66   from closely related rodent species.

67

68   *A genome-resolved bacterial phylogeny from the rodent gut microbiota*

69   Here, we employed comparative, genome-resolved metagenomics approaches to test for co-

70   diversification between GM strains and rodents, to assess the extent to which ancestral GM

71   symbionts have persisted within laboratory mice, and to test how natural selection and genetic

72   drift have driven divergence of LGM strains from their wild relatives. To enable tests for co-

73   diversification between gut microbiota and rodents in the super family Muroidea, we used a

74   combination of long-read Oxford Nanopore and short-read Illumina sequencing to generate 504

75   metagenome-assembled genomes (MAGs) from individuals of six species/subspecies of deer

76   mice (genus *Peromyscus*) descended from wild populations in the United States and reared in a

77   common facility on a common diet (Methods; Extended Data Table 1). We combined these

78   MAGs with previously published MAGs from the gut microbiota of 307 host individuals from 14

79   rodent species[1,2,5,19–28] (Fig. 1a; Extended Data Table 2) and generated a curated host tree from

80   timetree.org[29]. We used IQTree2[30] to construct a maximum likelihood phylogenetic tree of all

81   MAGs based on single-copy core genes (Methods), which define bacterial lineages' taxonomic

82   classifications[31]. The final tree included 5,567 MAGs from 20 rodent host species, allowing

83   assessment of GM-strain diversification coincident with rodent speciation.

84

85   *Widespread co-diversification between gut bacterial symbionts and rodents*

86   To test for co-diversification between GM strains and rodent species, we employed an approach

87   previously used to identify GM strains that co-diversified with primate species[10]. We tested

88   every node in the distal 1/4th of the bacterial phylogeny (1,245 nodes) for co-diversification with

89   host species using the method developed by Hommola *et al.*[32] (Methods), since previous

90   molecular clock analyses suggest that more basal nodes likely predate the most-recent common

91   ancestors of rodents[10]. We identified 158 gut bacterial clades showing evidence of co-

92   diversification with host species following previously employed significance thresholds of r >

93   0.75 and *p*-value < 0.01 (Extended Data Table 3, Fig. 1b)[10]. Co-diversifying gut bacterial

94   lineages comprised 22.6% of the total branch length on the MAG phylogeny and spanned 8

95   phyla. Perfect or near perfect concordance between host and symbiont phylogenies was

96   observed, indicative of ancestral relationships between host lineages and host species–specific

97   symbionts spanning > 25 million years (Fig. 1c–e, Extended Data Figure 1). These include

98   strains of *Helicobacter ganmani* (a common commensal of laboratory mice[33]), an unclassified

99   species of *Lactobacillus* (paralleling results from studies of this taxon in other hosts[34]), several

100   unclassified genera, and others (Extended Data Table 3). Interestingly, within these co-

101   diversifying clades, MAGs derived from laboratory mice formed sister clades to MAGs derived

102   from wild mice (*e.g.*, Fig. 1 c, e), 'wildlings'[5] (laboratory mice born to a wild-caught mother via

103   embryo transfer), and 'ex-wild' mice (wild-caught mice housed in the laboratory animal

104   facilities) (Extended Data Table 3). The phylogenetic relationships among LGM and WGM

105   strains indicate that LGM strains are descended from ancestral symbiont lineages that resided

106   within wild house mice and the common ancestors of wild house mice and other Muroidea

107   species.

108   To further assess the evidence for co-diversification in these clades, we conducted tests

109   after subsampling a single MAG from each monophyletic clade derived from a single host

110   species. These analyses assessed only the association between the backbone of each symbiont

111   clade and the host phylogeny, eliminating the possibility of pseudoreplication caused by repeated

112   sampling of individual bacterial clades from the same host species[35]. We employed multiple tests

113   for co-diversification, including PACo[36], ParaFit[37], and Hommola's test[32]. 324 clades displaying

114   significant evidence of co-diversification in at least one test (Extended Data Table 3, Extended

115   Data Figure 2), the results of these different tests were significantly associated with one another

116   (Extended Data Figure 2A–C), and 156 clades displayed significant evidence for co-

117   diversification based on at least two of the tests (Extended Data Figure 2D). We observed

118   between eight-fold and twelve-fold more significantly co-diversifying clades (based on a *p*-value

119   of 0.01) than expected under the null hypothesis (*i.e.*, 1% of tests) (Extended Data Figure 3),

120   depending on the specific test employed. In addition, we assessed the false discovery rate of the

121   initial scan for co-diversification based on the complete dataset using a previously developed

122   permutation test[10,38], finding that the scan based on the real data detected always detected more

123   co-diversifying clades than the number detected in the permuted scans, which averaged 53.74

124   clades (Extended Data Figure 3). Sensitivity analyses further indicated that the detection of 73–

125   100% of co-diversifying clades was robust to the removal of MAGs from individual host species

126   (depending on the host species removed) (Extended Data Figure 4), and molecular clock

127   analyses corroborated contemporaneous diversification of symbiont and rodent lineages

128   (Extended Data Figure 5, Extended Data Table 4). Cumulatively, these results demonstrate

129   widespread co-diversification between gut microbiota and rodent species.

130

131   *Retention and extinction of co-diversifying symbionts in laboratory house mice*

132   The discovery of co-diversifying GM strains enabled identification of ancestral GM lineages that

133   have either been retained in or lost from laboratory house mice. Of the 158 co-diversifying

134   clades identified, 40 phylogenetically independent (*i.e.*, non-nested) clades were inferred to be

135   ancestral to house mice and other murids (*i.e.*, present in *Mus musculus domesticus*, at least one

136   non-*M. m. domesticus* murid, and at least one outgroup to murids) (Supplementary Information).

137   Of these 40 ancestral clades, 24 contained MAGs from laboratory house mice (Fig. 1f, Extended

138   Data Figure 6). Previous work showed that wild-derived inbred mouse lines could retain subsets

139   of the microbiota from their wild population of origin for > 10 host generations[39]. The

140   observation of 24 ancestral, co-diversifying clades in laboratory mice (Fig. 1f) shows that these

141   symbioses have persisted since their hosts' derivation from wild stock > 100 years ago[13].

142   Our analyses also indicated that laboratory house mice have experienced elevated rates of

143   loss of ancestral symbionts relative to wild house mice. Only 7 ancestral clades lacked MAGs

144   from wild house mice, whereas 33 clades contained MAGs from wild house mice (compared to

145   16 and 24 clades, respectively, for laboratory house mice). These results indicate significantly

146   greater absence of these clades from laboratory house mice than from wild house mice (chi-

147   squared test *p*-value = 0.0262), consistent with accelerated loss of ancestral gut-microbiota

148   diversity from laboratory house mice[1]. This difference could not be explained by sampling effort,

149   which favored laboratory house mice (217 laboratory versus 90 wild house-mouse samples).

150   MAGs from 'wildling'[5] or 'rewilded'[3,4] mice (lab mice released outdoors) were contained within

151   a subset of clades lacking MAGs from laboratory mice (Extended Data Figure 6), indicating that

152   ancestral clades absent from laboratory mice can be regained through 'wildling' or 'rewilding'

153   approaches.

154

155   *Altered genomic signatures of positive selection in LGM strains*

156 Within co-diversifying clades ancestral to murids (Fig. 1f), LGM and WGM strains repeatedly

157 formed reciprocally monophyletic clades (*e.g.*, Fig. 1c, e), indicating their genomic

158 distinctiveness. We next interrogated the evolutionary forces that have driven this divergence.

159 We reasoned that LGM strains may be experiencing altered forces of natural selection compared

160 to their wild relatives due to inbred host genetic backgrounds, laboratory-mouse diets, and

161 myriad other factors. To test this idea, we conducted genome-wide scans for positive selection on

162 each protein-coding gene in each co-diversifying clade ancestral to murids that contained MAGs

163 from laboratory and wild house mice. For each gene, we calculated the ratio of the rates of

164 nonsynonymous and synonymous substitutions per site, *i.e.*, dN/dS, which is expected to be 1

165 under neutral evolution, >1 under positive selection to change the protein product, and < 1 under

166 purifying selection against non-synonymous mutations. Results showed that most co-diversifying

167 GM strains' genes have evolved under purifying selection in both wild and laboratory mice (Fig.

168 2, Extended Data Table 5), as expected. However, distinct sets of genes exhibited evidence of

169 positive selection in LGM and WGM strains (Fig. 2). Significantly more genes displayed dN/dS

170 > 1 in laboratory mice (76 genes) but dN/dS < 1 in wild mice than dN/dS > 1 in wild mice but

171 dN/dS < 1 in laboratory mice (50 genes) (binomial test p-value = 0.0255), consistent with novel

172 selective forces driving accelerated evolution of a minority of protein sequences encoded by the

173 genomes of LGM strains. Genes showing evidence of positive selection in the laboratory but

174 purifying selection (or near neutrality) in the wild included *hpt* (Borkfalkiaceae) involved in the

175 purine salvage pathway, *tsaD* (Muribaculaceae) involved in tRNA metabolism, *oppC*

176 (*Schaedlerella*) involved in oligopeptide transport, *kbl* (*Odoribacter*) involved in amino acid

177 degradation, *carB_2* (*Duncaniella freteri*) involved in pyrimidine metabolism, *pgi* (unclassified

178 genus 1XD8-76) involved in carbohydrate degradation, and *pflB* (*Lachnospira*) involved in

179   pyruvate fermentation (Fig. 2; Extended Data Table 5). Laboratory-specific positive selection on

180   these metabolic genes may result from the compositionally distinct, *ad libitum* diets of laboratory

181   mice, although our analyses were not able to identify specific selective agents. We also tested for

182   differences in gene functional annotations between laboratory and wild GM strains (and co-

183   diversifying and non-co-diversifying clades, Supplementary Information), but the left-skewed

184   distributions of p-values obtained indicated that these analyses lacked power (Extended Data

185   Table 6, S7, respectively), suggesting relatively greater applicability of sequence-based scans for

186   selection (*e.g.*, dN/dS) for MAGs. These results identify genes in ancestral, co-diversifying

187   symbionts of house mice showing evidence of laboratory-specific adaptation.

188

189   *Significantly elevated genetic drift in LGM strains*

190   In addition to testing for divergent natural selection between LGM and WGM strains, we also

191   tested for divergence in the strength of genetic drift. Laboratory breeding and animal care

192   procedures may exert bottlenecks on LGM strains, which would elevate the strength of genetic

193   drift. C57BL/6J—the most widely used laboratory mouse line—was derived from a single

194   mating pair (https://www.jax.org/strain/000664), and previous work has shown that moving wild

195   mice into the laboratory and establishing inbred lines is associated with a precipitous loss of GM

196   diversity[39], a hallmark of drift. Moreover, once in the laboratory, GM strains are vertically

197   inherited from mother to offspring within inbred mouse lines[39] through stochastic sampling

198   processes that can exert bottlenecks on GM diversity[40].

199   Theory predicts that stronger genetic drift will reduce the efficacy of purifying selection,

200   increasing the rate of fixation of weakly deleterious mutations. In bacterial lineages with low

201   effective population sizes (N_e), stochastic sampling leads to elevated genome-wide rates of

202 fixation of nonsynonymous substitutions (dN) that would otherwise be efficiently purged by

203 purifying selection in lineages with large N_e, elevating dN/dS genome-wide[41,42]. Whereas

204 elevated dN/dS values in individual genes can be driven by the action of positive selection,

205 elevated genome-wide dN/dS is indicative of reduced N_e and increased genetic drift[43].

206 To test whether co-diversifying GM strains in laboratory mice have experienced elevated

207 genetic drift, we compared genome-wide dN/dS values in LGM and WGM strains within each

208 co-diversifying clade ancestral to murids. We observed significant genome-wide elevation of

209 dN/dS in LGM strains in tests based on all genes (paired-test p-value = 0.000356) and in tests

210 based only on genes under purifying selection (bottom-left quadrant of Fig. 2) (paired t-test p-

211 value = 0.00511) (Fig. 3a). The genome-wide signatures of genetic drift became more evident

212 when individual co-diversifying clades were tested separately (Fig. 3b–d). Significantly elevated

213 dN/dS in LGM strains was observed in clades of *Schaedlerella* (class: Clostridia) (paired t-test

214 FDR-corrected p-values = 2.05e-07, all genes; 5.87e-06, genes under purifying selection) (Fig.

215 3b), unclassified Lachnospiraceae genus CAG-95 (paired t-test FDR-corrected p-values < 5.5e-

216 15) (Fig. 3c), *Anaerotingum* (class: Clostridia) (paired t-test FDR-corrected p-values = 0.00390

217 and 0.0228) (Fig. 3d), and others (Extended Data Table 5). Only one co-diversifying clade,

218 unclassified Oscillospiraceae UMGS1872, displayed significantly higher dN/dS in the wild than

219 in the laboratory (paired t-test p-value = 7.93e-05 and 4.51e-05). Unclassified Oscillospiraceae

220 were previously shown to be two of seven bacterial taxa found at significantly higher frequency

221 in laboratory mice than in wild mice (compared to 68 taxa found at significantly higher

222 frequency in wild mice)[1]. Larger census populations sizes of this taxon may buffer against

223 stronger genetic drift in the laboratory. Elevated genetic drift in LGM strains was not observed

224 for non-co-diversifying symbiont clades (Mantel's r < 0) (Supplementary Information; Extended

225   Data Table 8), indicating that elevated genetic drift in the laboratory has primarily affected co-

226   diversifying bacterial symbionts. Moreover, genome-wide dN/dS was significantly higher for co-

227   diversified clades (r > 0.75) than for non-co-diversified clades (r < 0) in both laboratory and wild

228   house mice (Supplementary Information, Extended Data Figure 7), further indicating stronger

229   genetic drift in co-diversifying compared to non-co-diversifying GM symbiont lineages.

230

231   *Co-diversified WGM strains out-compete related LGM strains in vivo*

232   The observations that co-diversified LGM strains show genomic evidence of both laboratory-

233   specific adaptation (Fig. 2) and elevated genetic drift (Fig. 3) raised two conflicting hypotheses

234   regarding the relative fitness of LGM and WGM strains. Laboratory-specific adaptation is

235   expected to increase the fitness of LGM strains compared to WGM relatives in the laboratory-

236   mouse environment. In contrast, elevated genetic drift (Fig. 3) is expected to reduce fitness via

237   the accelerated fixation of weakly deleterious mutations (*i.e.*, genetic load). To assess the net

238   consequences of these evolutionary forces in driving divergence between LGM and WGM

239   strains, we analyzed data from competition experiments in which the relative fitness of strains

240   was assessed directly in germ-free laboratory mice[5].

241   In these experiments, individual wildling (C57BL/6J harboring wild-derived microbiota),

242   laboratory (C57BL/6J from Jackson Laboratory), and germ-free (GF) (C57BL/6J from Taconic)

243   mice were sampled and co-housed in trios for 17 days[5]. We assessed the relative fitness of co-

244   diversified wildling- and laboratory mouse–specific GM lineages in germ-free mice, enabling

245   comparisons to previous analyses that assessed invasion ability of all GM taxa[5]. To test for the

246   relative fitness of LGM lineages from co-diversified taxa compared to closely related wildling

247   GM lineages, we identified all taxa that showed evidence of co-diversification with hosts (Fig.

248   1b; Extended Data Table 3) and were present in both wildling and laboratory experimental mice.

249   We then identified all ASVs within these taxa that were detected in either wildling or laboratory

250   mice, but not both, at day 0 (*i.e.*, ASVs that were unambiguously wildling– or laboratory mouse–

251   derived). Based on these ASVs, beta-diversity dissimilarities between wildling and laboratory

252   mice sampled at day-0 (before co-housing) and co-housed GF mice sampled from day 1 to day

253   17 indicated that wildling GM displayed significant competitive advantages over closely related

254   LGM (Fig. 4). These advantages were evident during the first half of the experiment (days 1–6)

255   and became more pronounced in the latter half of the experiment (days 7–14) (Fig. 4a, b;

256   Extended Data Table 9) (non-parametric permutation t-test *p*-values < 0.001). Longitudinal

257   relative abundances of wildling and laboratory-mouse ASVs within co-diversified genera

258   showed significant wildling advantage (Fig. 4c) (*p*-value < 0.05; t-test, difference in mean

259   abundance days 7–17). Wildling advantage was observed in *Anaerotignum* (*p*-value = 0.027),

260   which also showed genome-wide evidence of elevated genetic drift in the laboratory (Fig. 3d).

261   Analyses based on co-diversified taxa indicated stronger advantages for wildling-GM ASVs than

262   did analyses based on the complete dataset containing non-co-diversified taxa (Extended Data

263   Figure 8), and removing co-diversified taxa from the complete dataset reduced the observed

264   wildling competitive advantage (Supplementary Information). These results show that co-

265   diversified GM taxa displayed disproportionate (relative to non-co-diversified GM taxa)

266   advantages for wildling ASVs, supporting accelerated accumulation of genetic load in co-

267   diversified LGM strains.

268   In summary, we found that laboratory mice have retained > 25-million-year-old symbiont

269   lineages that co-diversified with rodent species, and that these ancestral laboratory-mouse

270   symbionts have experienced elevated levels of genetic drift during > 120 years of captivity. The

271   observation that LGM strains from ancestral, co-diversifying taxa display increased genetic load

272   (Fig. 3) provides an evolutionary basis for their reduced fitness when competed in germ-free

273   mice against relatives from wild mice (Fig. 4). These findings suggest that genetic drift—rather

274   than positive selection—has been the predominant evolutionary force driving divergence of

275   LGM from wild ancestors.

276
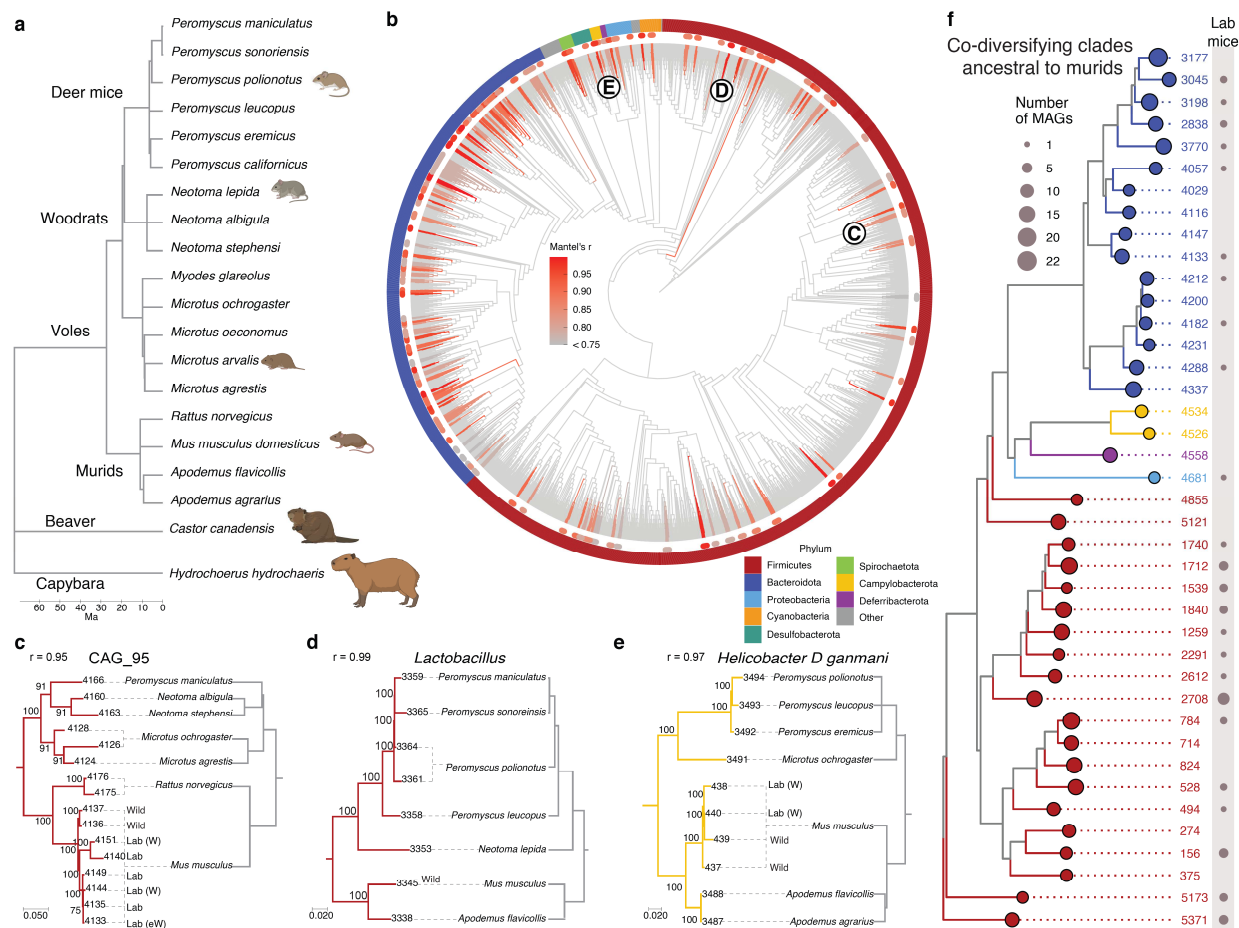
Fig. 1: Retention of ancestral, co-diversifying rodent gut symbionts in laboratory mice. a,
Phylogeny shows evolutionary relationships among rodent host species for which gut bacterial
genomes were included in this study. **b,** Phylogeny shows relationships among gut bacterial
genomes assembled from the rodent gut microbiota. Colors denote bacterial phyla. Bars
surrounding phylogeny mark clades displaying significant evidence of co-diversification ($r >$
0.75, p-value < 0.01). **c–e,** Tanglegrams show concordance between gut bacterial (left) and
rodent (right) phylogenetic trees. Dashed lines connect bacterial genomes with the host species
from which they were recovered. Genomes derived from mice (*Mus musculus*) sampled in the
lab or the wild are labeled. 'W' and 'eW' indicate 'wildling' and 'ex-wild' mice, respectively.
Numbers left and right of tree are bootstrap support values and genome IDs, respectively. **f,**

287   Phylogeny shows relationships among all bacterial genomes belonging to co-diversifying clades

288   shown in Fig. 1 that contain genomes from murids and non-murids, *i.e.*, co-diversifying clades

289   that could be inferred to be ancestral to murids. Circles indicate clades (colored by phylum, left)

290   or MAGs derived from laboratory mice (grey, right). Sizes of circles indicate the number of

291   MAGs. Identification numbers are listed to the right of each clade.

292

293

294
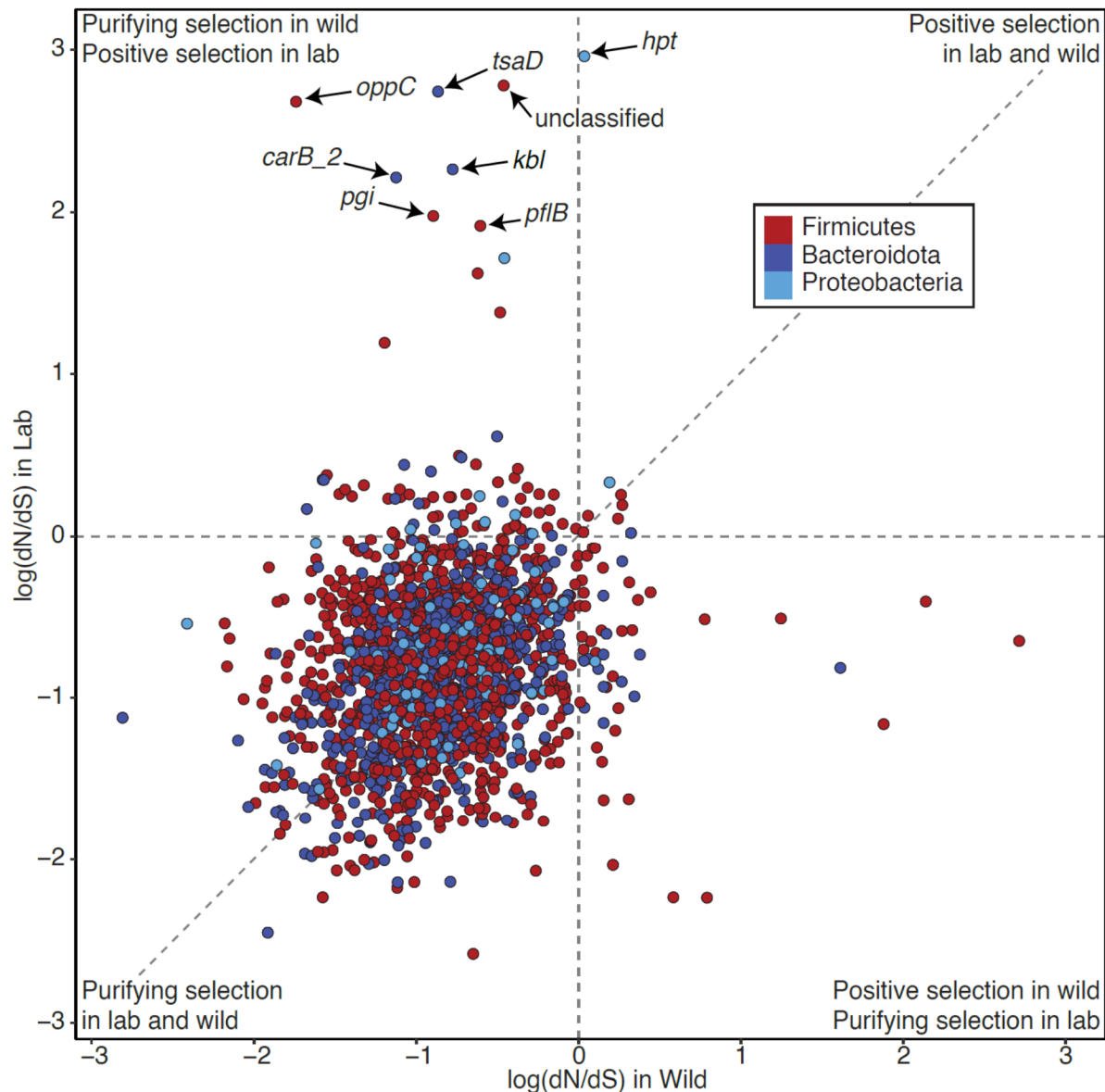
Fig. 2: Divergent positive selection on ancestral GM symbiont strains in wild and

laboratory mice. Scatter plot shows the log of the dN/dS ratio for bacterial genes in co-

diversifying clades in laboratory house mice (y-axis) and other rodents (x-axis). Each point

represents a bacterial gene. Positive values indicate evidence of positive selection, values near

zero indicate neutral evolution, and negative values indicate purifying/negative selection. Points

in the upper left quadrant show evidence of positive selection in laboratory house mice but

purifying/negative selection in other rodents.

302
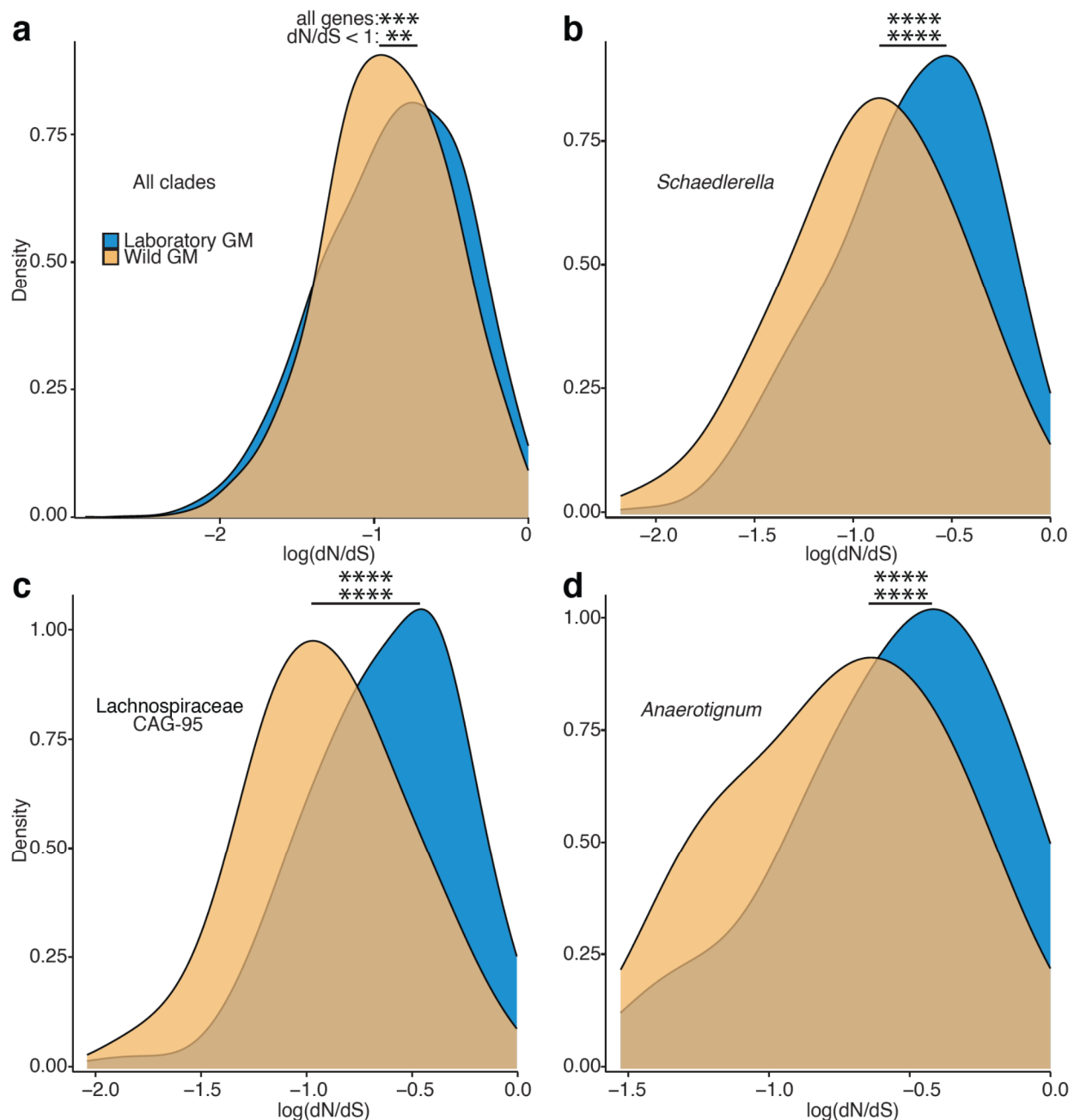
Fig. 3: Elevated mutational load in co-diversified LGM strains compared to WGM

relatives. a, Density plot shows significant genome-wide elevation of dN/dS (a hallmark of

genetic drift) in co-diversifying GM strains in laboratory house mice relative to wild house mice.

dN/dS values for all genes from all co-diversifying clades ancestral to murids and containing

MAGs from both laboratory and wild mice are shown. **b–d,** Density plots show significant

308   genome-wide elevation of dN/dS in individual co-diversifying clades in laboratory house mice

309   relative to wild house mice. In **a–d**, significance of paired t-tests for differences in mean is

310   denoted by asterisks; ** p-value < 0.01; *** p-value < 0.001; **** p-value < 0.0001. Top

311   asterisks denote significance of tests considering all genes, and bottom asterisks denote

312   significance of tests considering only genes displaying dN/dS < 1 (log dN/dS < 0) in both

313   laboratory and wild mice.

314
315

316
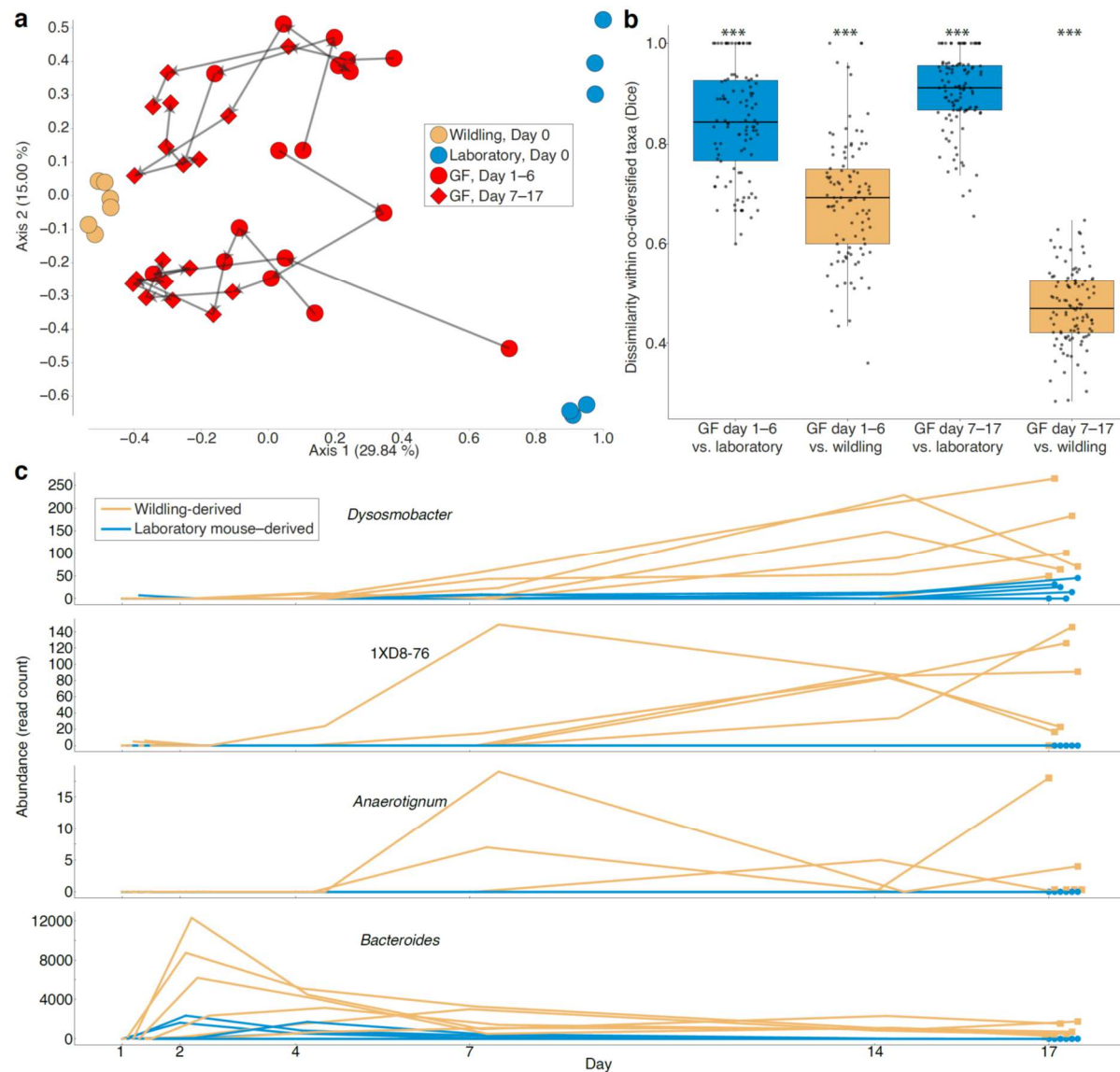
Fig. 4. Reduced *in vivo* fitness of co-diversified LGM strains compared to WGM relatives.

a, Principal coordinates plot shows beta-diversity (Dice) dissimilarities among microbiota

profiles based on laboratory mouse– and wildling-specific ASVs within co-diversified taxa.

Points are colored based on host of origin as indicated in the key (GF = ex-germ-free mice).

Arrows connect longitudinal samples from the same germ-free mouse. **b**, Boxplots show that ex-

germ-free mice harbored significantly more wildling-derived ASVs than laboratory mouse–

derived ASVs within co-diversified taxa. Asterisks indicate significant differences of boxplot

324   from all other groups based on permutation tests; *** *p*-value < 0.001. Significance testing was

325   conducted after averaging values of longitudinal samples from individual mice within each

326   group. **c**, Line plots show higher abundance of wildling-derived ASVs (yellow) compared to

327   laboratory mouse–derived ASVs (blue) within four bacterial genera showing evidence of co-

328   diversification (Fig. 1). Each line indicates the relative abundance of wildling-derived or

329   laboratory mouse–derived ASVs from each genus within individual ex-germ-free mice between

330   days 1 and 17. Data for other taxa are presented in Extended Data Table 10.

Methods

Ethical statement

All procedures conformed to guidelines established by the U.S. National Institutes of Health and have been approved by the Cornell University Institutional Animal Care and Use committee (IACUC: Protocol #2015-0060).

Sampling of Peromyscus gut microbiota

Samples from *Permoyscus* species sequenced in this study were collected from the University of South Carolina *Peromyscus* Stock Center. Host species sampled included *P. maniculatus bardii* (n=1), *P. leucopus* (n=1), *P. polionotus* (n=2), *P. errimicus* (n=1), *P. californicus* (n=1), and *P. maniculatus sonoriensis* (n=1). Each host lineage was reared in a common laboratory environment on a standard laboratory chow diet. No host lineage was rederived under sterile conditions (*e.g.*, through embryo transfer to a laboratory mouse lineage). These husbandry practices have been previously shown to enable the retention of wild-derived gut microbiota in the laboratory animal-facility environment for > 10 host generations[39]. For sampling, individual rodents were transferred to clean cages and monitored for 1-2 hours, after which fecal samples deposited during that time were collected with sterile tweezers. Fecal samples were immediately placed in empty sterile tubes on dry ice and shipped to Cornell University, where they were stored at -80C until DNA extraction.

DNA extraction and library preparation

For *Peromyscus* samples sequenced in this study, DNAs were extracted for Nanopore sequencing using a three-step extraction protocol. Steps included 1) osmotic lysis, 2) enzymatic

354   lysis, and 3) bead beating following previously described methods[10]. For each extraction,

355   ~100mg of starting fecal material was used to ensure sufficient yield for Nanopore sequencing.

356   Libraries were prepared using the Nanopore Ligation Sequencing kit (SQK-LSK110) following

357   the manufacturer-supplied protocols. Separate extractions from the same fecal samples were

358   made for Illumina short-read metagenome sequencing using Qiagen PowerSoil microbiome

359   extraction kits.

360

361   *Illumina metagenome sequencing*

362   Libraries for Illumina short-read metagenome sequencing of *Peromyscus* samples were prepared

363   at the Cornell Biotechnology Resource Center (BRC) using their Illumina TruSeq-equivalent

364   ligation library prep protocol (https://www.biotech.cornell.edu/). Libraries were sequenced on an

365   Illumina NovaSeq sequencer at the UC Davis DNA Technologies Core.

366

367   *Nanopore sequencing and base calling*

368   Each library was sequenced on the MinION platform using an entire flow cell. Base calling was

369   conducted either in real time or post-sequencing with the Guppy base caller[44] v3.1.5 using two

370   nVIDIA RTX 3090 Graphical Processing Units (GPUs). The following settings were employed

371   in guppy_basecaller --device "cuda:all" --chunk_size 3000 --chunks_per_runner 768 --

372   gpu_runners_per_device 4 --qscore_filtering --min_qscore 7 --config

373   dna_r9.4.1_450bps_hac.cfg --calib_detect --compress_fastq --recursive.

374

375   *Assembly of Peromyscus MAGs*

376   Contiguous sequences from *Peromyscus* MAGs were assembled from nanopore sequence data

377   and polished with Illumina short-read sequencing data using the snakemake[45] reticulatus

378   workflow available at https://github.com/SamStudio8/reticulatus. We used the MetaFlye v2.8

379   'spell' within reticulatus[46], followed by a polishing pipeline employing four rounds of polishing

380   by Racon[47], one round of Medaka v1.0.1 [https://github.com/nanoporetech/medaka], and two

381   rounds of Pilon v1.23 polishing with Illumina short-read metagenome data[48]. Finally, contigs

382   likely to be derived from hosts were removed from the polished assembly using the

383   'dehumanizer' step of the reticulatus pipeline against an assembly from the corresponding host

384   species (*P. leucopus*: GCA_004664715.1; *P. polionotus*: GCA_003704135.2; *P. maniculatus*:

385   GCA_003704035.1; *P. californicus*: GCA_007827085.2). Assembled and polished contigs were

386   binned in Anvi'o v6.2 using CONCOCT[49] and refined manually using anvi-summarize and anvi-

387   refine[50].

388

389   *Phylogenomic analyses*

390   Phylogeny was constructed from the combined set of MAGs from all host species for which > 20

391   MAGs were available as well as MAGs from *Castor canadensis*, for which only 16 MAGs were

392   available but which represents a basally branching rodent lineage that was not otherwise

393   represented in the data. Core genes from the bac120 collection were identified for each MAG in

394   GTDB-Tk v1.4.1 using the 'identify' function[31]. Concatenated core genes were then aligned in

395   GTDB-Tk using the 'align' function with default settings[31]. The alignment was then used to infer

396   a phylogenetic tree of the combined set of rodent MAGs in IQTree2 version 2.1.3 using the

397   settings -mset LG,WAG, --seed 0, and -B 1000.

398

399   *Scans for co-diversification*

400   To identify co-diversified clades in the rodent MAG phylogeny, we employed an extension of

401   the method developed by Hommola et al.[32], which uses permutation tests to estimate non-

402   parametric p-values based on the null hypothesis of no association between the symbiont and

403   host evolutionary distances. This workflow yielded a Mantel's r correlation coefficient for each

404   clade of gut bacteria tested as well as a non-parametric *p*-value indicating the probability of

405   observing by chance a Mantel's r greater than or equal to that observed in the real data.

406   Here, we applied these tests to nodes that contained ≥ 3 hosts and ≥ 7 symbionts, and spanned

407   less than 1/4th of the total bacterial phylogeny, as we reasoned that more deeply diverging clades

408   represent bacterial diversification events that predate the most recent common ancestor of

409   rodents. For each node, the test employed 999 permutations. Only clades with a resulting p-value

410   of < 0.01 and an r coefficient > 0.75 were considered "co-diversifying" for downstream analyses.

411   All code used to conduct these analyses is available in Python at

412   https://github.com/CUMoellerLab/codiv-tools and in R at

413   https://github.com/DanielSprockett/codiv.

414   In addition, we conducted scans for co-diversification based on dereplicated clades

415   containing only a single MAG per monophyletic clade of MAGs derived from the same host

416   species. For these tests, we randomly selected a MAG from each monophyletic clade and

417   performed PACo[36], ParaFit[37], and Hommola's test[32] using default settings. All code used for

418   these analyses is available at https://github.com/DanielSprockett/codiv.

419

420   *Permutation tests for whether extent of co-diversification exceeds null expectation*

421   In some cases, the MAG clades tested in the co-diversification scan were non-independent due to

422   the underlying tree structure, complicating the adjustment of p-values based on false discovery

423   rate correction. Moreover, in some cases MAGs belonging to the same co-diversifying clade

424   were sampled from multiple individuals per host species, thereby introducing pseudo-replication

425   into tests for co-diversification between host-species lineages. To address these issues and to

426   assess whether there was greater evidence for co-diversification of MAG clades with rodent

427   species in the MAG phylogeny than expected by chance, we conducted additional permutation

428   tests in which the host-species labels were permuted on the host-species phylogeny 100 times

429   and the co-diversification scans were reperformed for each permutation. These analyses yielded

430   a null distribution of the proportion of co-diversifying clades expected to reach significance

431   thresholds ($r > 0.75$, p-value < 0.01) by chance given the underlying structure of and

432   pseudoreplication in the MAG phylogeny. This null distribution was used to calculate a non-

433   parametric p-value indicating the probability of observing, by chance under the null hypothesis

434   of no association between bacterial and host evolutionary distances, a number of significantly co-

435   diversifying clades ($r > 0.75$, p-value < 0.01) that was equal to or greater than the number

436   observed in the analyses based on the host phylogeny containing the correct host-species tip

437   labels. All code used to conduct these analyses is available in Python at

438   https://github.com/CUMoellerLab/codiv-tools and in R at

439   https://github.com/DanielSprockett/codiv.

440

441   *Molecular clock analyses*

442   We regressed symbiont divergence estimates based on protein-sequence divergence in clades

443   that displayed the strongest evidence of co-diversification (that is, Mantel's $r > 0.95$) and known

444   divergence times of host species based on timetree.org[29]. These regression analyses and

445   calculations of 95% confidence intervals were conducted in base R (version 4.2.3).

446

447   *Phylogenetic ANOVA*

448   Phylogenetic ANOVA was performed using the rodent gut bacterial phylogeny and the KEGG

449   annotations for each MAG to identify gene annotations enriched in co-diversifying clades

450   relative to non-co-diversifying clades or in laboratory-mouse symbionts relative to wild-mouse

451   symbionts. Theses analyses were conducted using the phylANOVA function in the R package

452   'phytools'[51] v2.1. Benjamin-Hochberg correction was performed to account for multiple testing

453   across classes of annotations.

454

455   *dN/dS analyses*

456   For each co-diversifying clade containing MAGs from laboratory and wild house mice, we used

457   Roary[52] v3.12.0 to identify and codon-align each gene family containing orthologs from at least

458   one laboratory-derived house-mouse MAG and at least one wild-derived house-mouse MAG.

459   Codon alignments were then used to construct a phylogenetic tree for each gene family using

460   RAxM[53] v8.2.12. Codon alignments and gene trees were then used in CODEML within PAML[54]

461   v4.10.6 to estimate the proportion of nonsynonymous substitutions per nonsynonymous site (dN)

462   to synonymous substitutions per synonymous site (dS) (*i.e.*, dN/dS) for every branch leading to a

463   laboratory-derived house-mouse gene copy and every branch leading to a wild-derived house-

464   mouse gene copy. The averages for laboratory-derived house-mouse gene copies and wild-

465   derived house-mouse gene copies were calculated for each gene family. Differences in genome-

466   wide dN/dS across the whole dataset and in individual clades were conducted with paired t-tests

467   in base R. All genes with nonzero dN and dS are shown in Figs. 2 and 3.

468

469   *Reanalysis of co-housing experiments*

470   We downloaded fastq files from accessions from PRJNA540893[5], which contained results of an

471   experiment in which C57BL/6J mice from the Jackson Laboratory (a source from which

472   genomes of laboratory-mouse GM strains displaying evidence of genetic drift were assembled,

473   *e.g.*, Fig. 3) containing either a laboratory-derived or wild-derived microbiota were co-housed

474   with germ-free mice for 17 days. Sequences were denoised with dada2[55] in qiime2[56] v2023.9

475   using the following settings: --p-trim-left 0 --p-trunc-len 200. GTDB ribosomal sequences and

476   taxonomy (bac120_ssu_reps.fna.gz and bac120_taxonomy.tsv) were imported into qiime using

477   'qiime tools import', and a classifier was trained using 'qiime feature-classifier fit-classifier-

478   naive-bayes'[57]. ASVs were then classified using 'qiime feature-classifier classify-sklearn'[57].

479   Samples were rarefied to a common depth of 40,000 reads (results were qualitatively identical

480   with and without rarefaction). A total of 2,640 ASVs were present in the final complete dataset.

481   Diagnostic ASVs belonging to co-diversifying taxa and found in either wildling or laboratory

482   mice at experimental day 0 (105 ASVs) were retained using 'qiime feature-table filter-features'.

483   Wildling and laboratory-mouse samples at day zero and GF-mouse samples from days 1–17

484   were retained with 'qiime feature-table filter-samples'. Dice dissimilarities (to assess strain

485   sharing) among diagnostic ASV profiles were calculated with 'qiime diversity beta'. Principal

486   Coordinates Analyses (PCoA) were conducted using 'qiime diversity pcoa' and plots were

487   generated using 'qiime emperor plot'[58]. Boxplots were created in R using ggplot2 (Version

488   3.5.1).

References

1. Bowerman, K. L. *et al.* Effects of laboratory domestication on the rodent gut microbiome. *ISME Commun.* **1**, 49 (2021).

2. Rosshart, S. P. *et al.* Wild mouse gut microbiota promotes host fitness and improves disease resistance. *Cell* **171**, 1015-1028.e13 (2017).

3. Chen, Y.-H. *et al.* Rewilding of laboratory mice enhances granulopoiesis and immunity through intestinal fungal colonization. *Sci. Immunol.* **8**, eadd6910 (2023).

4. Yeung, F. *et al.* Altered immunity of laboratory mice in the natural environment is associated with fungal colonization. *Cell Host Microbe* **27**, 809-822.e6 (2020).

5. Rosshart, S. P. *et al.* Laboratory mice born to wild mice have natural microbiota and model human immune responses. *Science* **365**, eaaw4361 (2019).

6. Groussin, M. *et al.* Unraveling the processes shaping mammalian gut microbiomes over evolutionary time. *Nat. Commun.* **8**, 14319 (2017).

7. Levin, D. *et al.* Diversity and functional landscapes in the microbiota of animals in the wild. *Science* **372**, (2021).

8. Suzuki, T. A. *et al.* Codiversification of gut microbiota with humans. *Science* **377**, 1328–1332 (2022).

9. Moeller, A. H. *et al.* Dispersal limitation promotes the diversification of the mammalian gut microbiota. *Proc. Natl. Acad. Sci.* **114**, 13768–13773 (2017).

10. Sanders, J. G. *et al.* Widespread extinctions of co-diversified primate gut bacterial symbionts from humans. *Nat. Microbiol.* 1–12 (2023).

11. Ley, R. E. *et al.* Evolution of mammals and their gut microbes. *Science* **320**, 1647–1651 (2008).

12. Moeller, A. H. *et al.* Cospeciation of gut microbiota with hominids. *Science* **353**, 380–382 (2016).

13. Beck, J. A. *et al.* Genealogies of mouse inbred strains. *Nat. Genet.* **24**, 23–25 (2000).

14. McCutcheon, J. P. & Moran, N. A. Extreme genome reduction in symbiotic bacteria. *Nat. Rev. Microbiol.* **10**, 13–26 (2012).

15. Perreau, J. & Moran, N. A. Genetic innovations in animal–microbe symbioses. *Nat. Rev. Genet.* **23**, 23–39 (2022).

519   16. Groussin, M., Mazel, F. & Alm, E. J. Co-evolution and co-speciation of host-gut bacteria
520   systems. *Cell Host Microbe* **28**, 12–22 (2020).

521   17. Parks, D. H. *et al.* Recovery of nearly 8,000 metagenome-assembled genomes substantially
522   expands the tree of life. *Nat. Microbiol.* **2**, 1533–1542 (2017).

523   18. Bickhart, D. M. *et al.* Generating lineage-resolved, complete metagenome-assembled
524   genomes from complex microbial communities. *Nat. Biotechnol.* **40**, 711–719 (2022).

525   19. Donovan, M. *et al.* Metagenome-assembled genome sequences of five strains from the
526   *Microtus ochrogaster* (prairie vole) fecal microbiome. *Microbiol. Resour. Announc.* **9**, e01310-
527   19 (2020).

528   20. Kohl, K. D. *et al.* Metagenomic sequencing provides insights into microbial detoxification in
529   the guts of small mammalian herbivores (*Neotoma* spp.). *FEMS Microbiol. Ecol.* **94**, (2018).

530   21. Kohl, K. D., Weiss, R. B., Cox, J., Dale, C. & Dearing, M. D. Gut microbes of mammalian
531   herbivores facilitate intake of plant toxins. *Ecol. Lett.* **17**, 1238–1246 (2014).

532   22. Xiao, L. *et al.* A catalog of the mouse gut metagenome. *Nat. Biotechnol.* **33**, 1103–1108
533   (2015).

534   23. Wang, J. *et al.* Dietary history contributes to enterotype-like clustering and functional
535   metagenomic content in the intestinal microbiome of wild mice. *Proc. Natl. Acad. Sci.* **111**,
536   E2703–E2710 (2014).

537   24. Pan, H. *et al.* A gene catalogue of the Sprague-Dawley rat gut metagenome. *Gigascience* **7**,
538   giy055 (2018).

539   25. Zhao, L. *et al.* Saturated long-chain fatty acid-producing bacteria contribute to enhanced
540   colonic motility in rats. *Microbiome* **6**, 107 (2018).

541   26. Zhang, S. *et al.* Shen-Ling-Bai-Zhu-San alleviates functional dyspepsia in rats and modulates
542   the composition of the gut microbiota. *Nutr. Res.* **71**, 89–99 (2019).

543   27. Finlayson-Trick, E. C. L. *et al.* Taxonomic differences of gut microbiomes drive cellulolytic
544   enzymatic potential within hind-gut fermenting mammals. *PLoS ONE* **12**, e0189404 (2017).

545   28. Hildebrand, F. *et al.* A comparative analysis of the intestinal metagenomes present in guinea
546   pigs (*Cavia porcellus*) and humans (*Homo sapiens*). *BMC Genom.* **13**, 514 (2012).

547   29. Kumar, S. *et al.* TimeTree 5: An expanded resource for species divergence times. *Mol. Biol.*
548   *Evol.* **39**, msac174 (2022).

549   30. Minh, B. Q. *et al.* IQ-TREE 2: New models and efficient methods for phylogenetic inference
550   in the genomic era. *Mol. Biol. Evol.* **37**, 1530–1534 (2020).

31. Chaumeil, P.-A., Mussig, A. J., Hugenholtz, P. & Parks, D. H. GTDB-Tk: a toolkit to classify genomes with the Genome Taxonomy Database. *Bioinformatics* **36**, 1925–1927 (2020).

32. Hommola, K., Smith, J. E., Qiu, Y. & Gilks, W. R. A permutation test of host–parasite cospeciation. *Mol. Biol. Evol.* **26**, 1457–1468 (2009).

33. Robertson, B. R., O'Rourke, J. L., Vandamme, P., On, S. L. & Lee, A. *Helicobacter ganmani* sp. nov., a urease-negative anaerobe isolated from the intestines of laboratory mice. *Int. J. Syst. Evol. Microbiol.* **51**, 1881–1889 (2001).

34. Li, F. *et al.* A phylogenomic analysis of *Limosilactobacillus reuteri* reveals ancient and stable evolutionary relationships with rodents and birds and zoonotic transmission to humans. *BMC Biol.* **21**, 53 (2023).

35. Nishida, A. H. & Ochman, H. Captivity and the co-diversification of great ape microbiomes. *Nat. Commun.* **12**, 5632 (2021).

36. Hutchinson, M. C., Cagua, E. F., Balbuena, J. A., Stouffer, D. B. & Poisot, T. paco: implementing procrustean approach to cophylogeny in R. *Methods Ecol. Evol.* **8**, 932–940 (2017).

37. Paradis, E. & Schliep, K. ape 5.0: an environment for modern phylogenetics and evolutionary analyses in R. *Bioinformatics* **35**, 526–528 (2018).

38. Moeller, A. H., Sanders, J. G., Sprockett, D. D. & Landers, A. Assessing co-diversification in host-associated microbiomes. *J. Evol. Biol.* (2023).

39. Moeller, A. H., Suzuki, T. A., Phifer-Rixey, M. & Nachman, M. W. Transmission modes of the mammalian gut microbiota. *Science* **362**, 453–457 (2018).

40. Sonnenburg, E. D. *et al.* Diet-induced extinctions in the gut microbiota compound over generations. *Nature* **529**, 212–215 (2016).

41. Kuo, C.-H., Moran, N. A. & Ochman, H. The consequences of genetic drift for bacterial genome complexity. *Genome Res.* **19**, 1450–1454 (2009).

42. Ohta, T. The nearly neutral theory of molecular evolution. *Annu. Rev. Ecol. Syst.* **23**, 263–286 (1992).

43. Daubin, V. & Moran, N. A. Comment on "The origins of genome complexity." *Science* **306**, 978 (2004).

44. Wick, R. R., Judd, L. M. & Holt, K. E. Performance of neural network basecalling tools for Oxford Nanopore sequencing. *Genome Biol.* **20**, 129 (2019).

45. Mölder, F. *et al.* Sustainable data analysis with Snakemake. *F1000Res.* **10**, 33 (2021).

583   46. Kolmogorov, M. *et al.* metaFlye: scalable long-read metagenome assembly using repeat
584   graphs. *Nat. Methods* **17**, 1103–1110 (2020).

585   47. Vaser, R., Sović, I., Nagarajan, N. & Šikić, M. Fast and accurate de novo genome assembly
586   from long uncorrected reads. *Genome Res.* **27**, 737–746 (2017).

587   48. Walker, B. J. *et al.* Pilon: an integrated tool for comprehensive microbial variant detection
588   and genome assembly improvement. *PLoS ONE* **9**, e112963 (2014).

589   49. Alneberg, J. *et al.* Binning metagenomic contigs by coverage and composition. *Nat. Methods*
590   **11**, 1144–1146 (2014).

591   50. Eren, A. M. *et al.* Community-led, integrated, reproducible multi-omics with anvi'o. *Nat.*
592   *Microbiol.* **6**, 3–6 (2021).

593   51. Revell, L. J. phytools 2.0: an updated R ecosystem for phylogenetic comparative methods
594   (and other things). *PeerJ* **12**, e16505 (2024).

595   52. Page, A. J. *et al.* Roary: rapid large-scale prokaryote pan genome analysis. *Bioinformatics*
596   **31**, 3691–3693 (2015).

597   53. Stamatakis, A. RAxML version 8: a tool for phylogenetic analysis and post-analysis of large
598   phylogenies. *Bioinformatics* **30**, 1312–1313 (2014).

599   54. Yang, Z. PAML 4: Phylogenetic Analysis by Maximum Likelihood. *Mol. Biol. Evol.* **24**,
600   1586–1591 (2007).

601   55. Callahan, B. J. *et al.* DADA2: High-resolution sample inference from Illumina amplicon
602   data. *Nat. Methods* **13**, 581–583 (2016).

603   56. Bolyen, E. *et al.* Reproducible, interactive, scalable and extensible microbiome data science
604   using QIIME 2. *Nat. Biotechnol.* **37**, 852–857 (2019).

605   57. Bokulich, N. A. *et al.* Optimizing taxonomic classification of marker-gene amplicon
606   sequences with QIIME 2's q2-feature-classifier plugin. *Microbiome* **6**, 90 (2018).

607   58. Vázquez-Baeza, Y., Pirrung, M., Gonzalez, A. & Knight, R. EMPeror: a tool for visualizing
608   high-throughput microbial community data. *Gigascience* **2**, 16 (2013).

609

610   **Acknowledgements**

616 **Author information**

617 *Contributions*

618 A.H.M. supervised the research, performed analyses, and wrote and edited the paper. D.D.S.

619 performed analyses and wrote and edited the paper. A.A.L., B.A.D., and J.G.S. performed

620 analyses and edited the paper.

621 **Corresponding author**

622 Correspondence to Andrew H. Moeller, andrew.moeller@princeton.edu.

623 **Ethics declarations**

624 *Competing interests*

625 The authors declare no competing interests.

626 **Data availability**

627 All sequence data generated in this study have been deposited to the National Center for

628 Biotechnology Information Sequence Read Archive under accessions BioProject ID

629 PRJNA1089132. Additional metadata about the genome assemblies generated by previous

630 studies are available at doi.org/10.1038/s43705-021-00053-9.

631   **Extended Data Figures**

632   **Extended Data Figure 1**

633
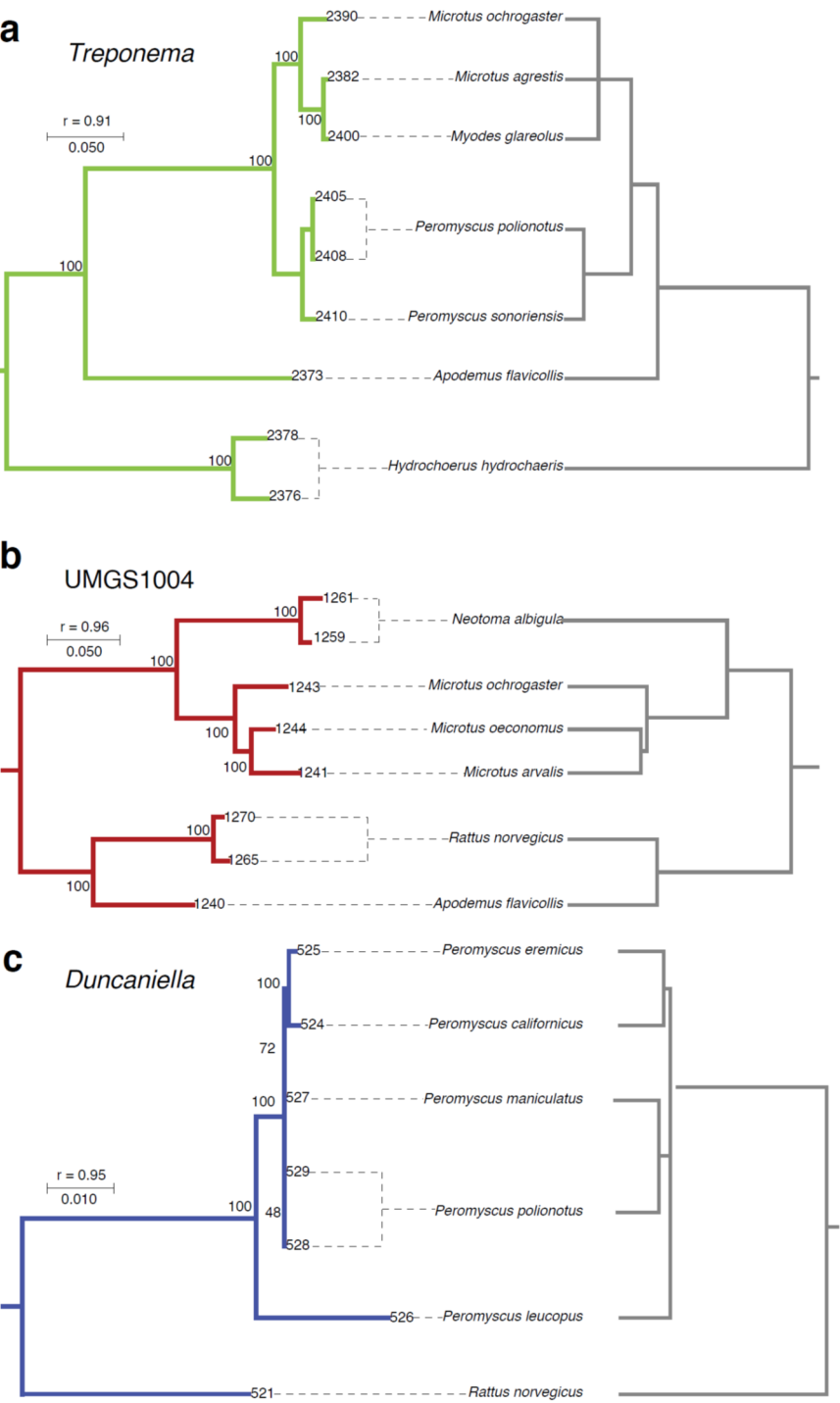
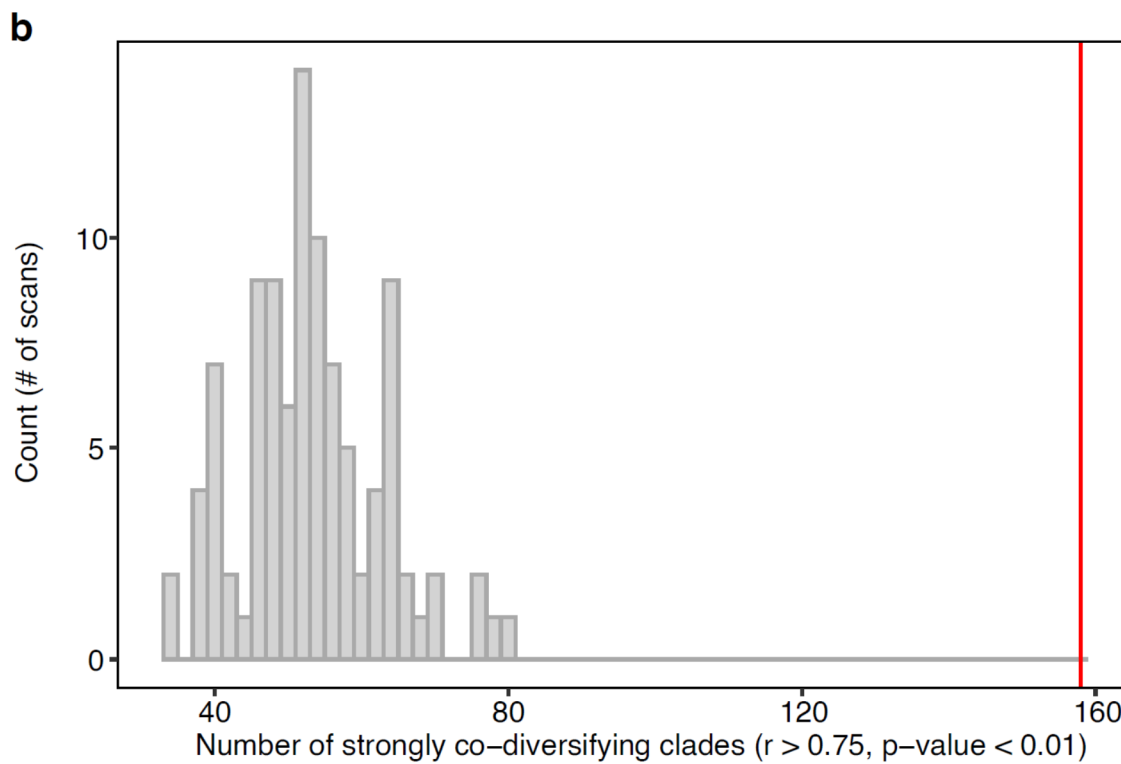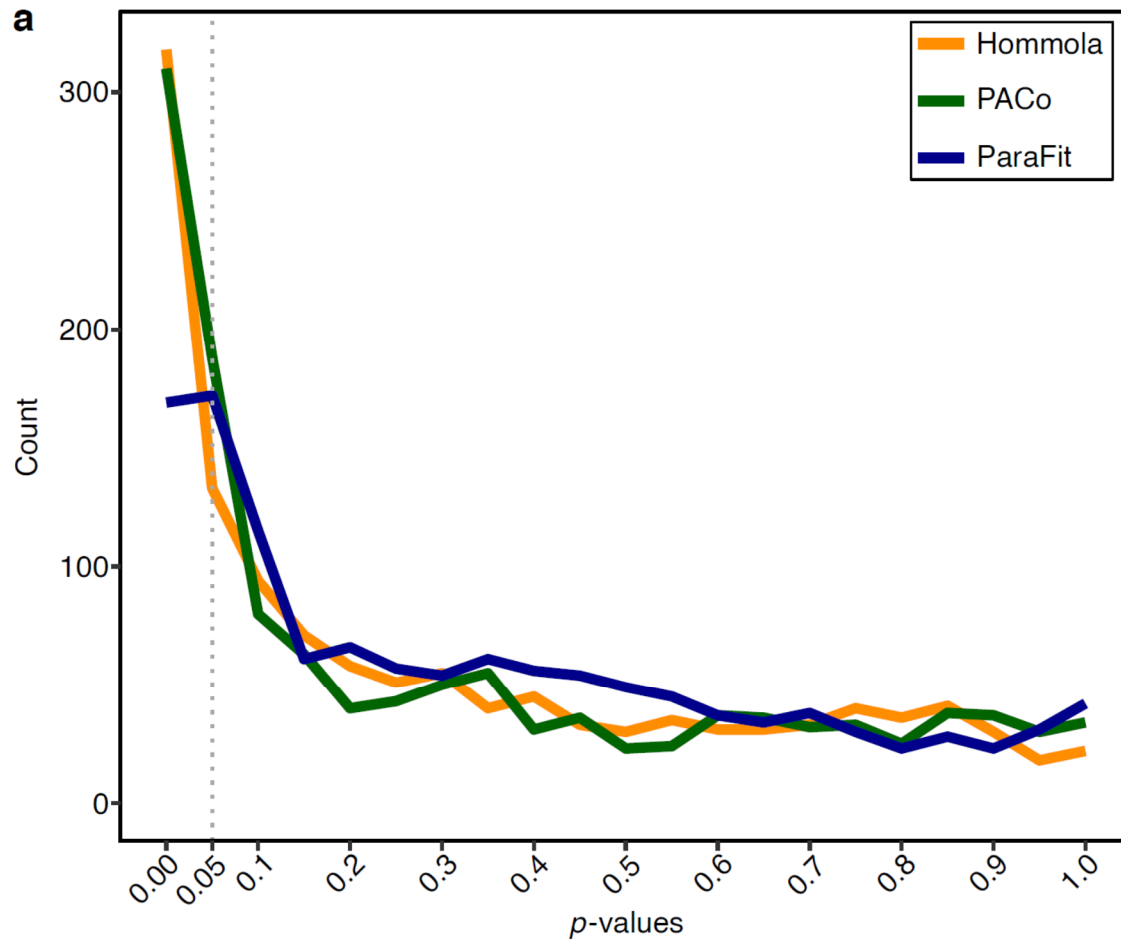634   **Extended Data Figure 1: Examples of co-diversifying clades lacking MAGs from house**

635   **mice. a–c,** Trees show phylogenetic relationships among symbiont MAGs (left) and the rodent

636   host species from which they were recovered (right). Symbiont branches are colored by phylum

637   as in Fig. 1. Dashed lines connect MAGs to the host species from which they were recovered.

638   The test statistic from the Hommola test (r) for each clade is shown. Branch lengths correspond

639   to amino acid substitutions per site.

640
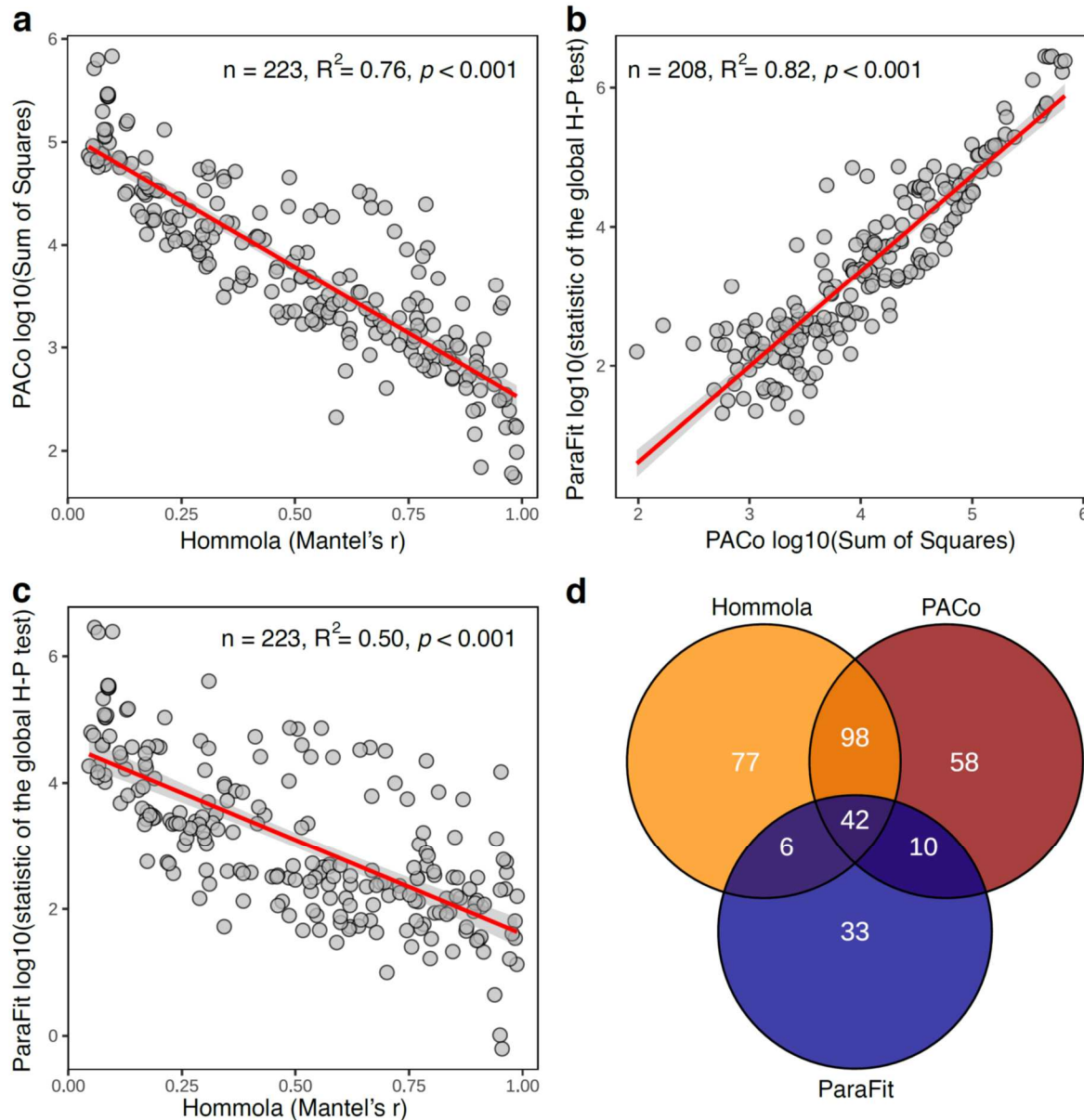
Extended Data Figure 2: Comparisons of tests for co-diversification based on de-replicated (*i.e.*, collapsed) tests. a–c, Scatter plots show relationships of test statistics between pairs of tests for co-diversification based on clades subsampled to a single MAG per host species. Tests include Hommola, PACo, and ParaFit. Red lines indicate best-fit regressions, and shaded gray areas represent 95% confidence bands. **d,** Venn diagram shows overlap between significant clades obtained from the three different tests employed.

649   **Extended Data Figure 3: Evidence for co-diversification from each class of tests exceeds**

650   **that expected under the null hypotheses. a,** Lines show distributions of p-values obtained from

651   scans of co-diversification based on down-sampled clades (*i.e.*, down sampled to contain one

652   MAG per host species) for PACo, ParaFit, and Hommola tests. **b,** Histogram shows the number

653   of co-diversifying clades detected (r > 0.75, p-value < 0.01) based on Hommola scans of the

654   entire MAG phylogeny and permuted host-species tip labels. Vertical red line indicates the

655   number of co-diversifying clades detected in the scan based on the real data (*i.e.*, non-permuted

656   host-species tip labels).

657

658
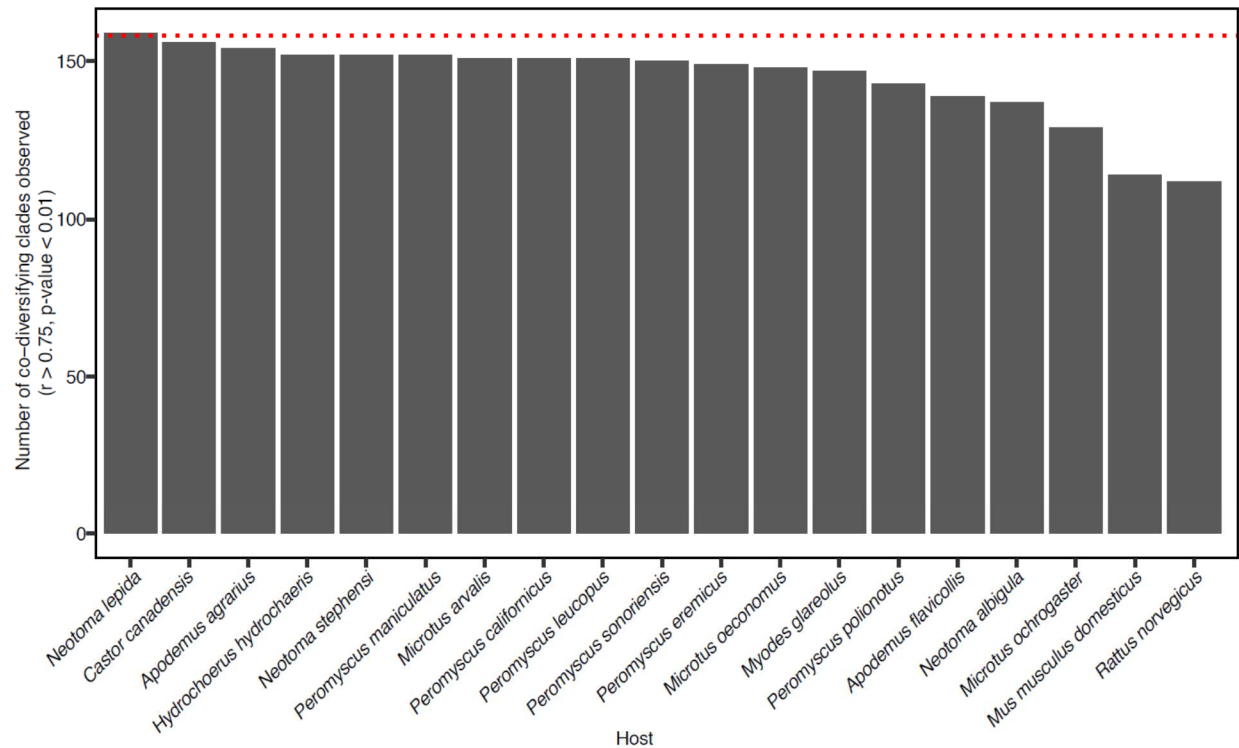
**Extended Data Figure 4: Sensitivity analyses of Hommola scans for co-diversification based on the complete dataset.** Barplot shows the number of strongly co-diversifying clades (r > 0.75, *p*-value < 0.01) detected based on sensitivity analyses in which scans for co-diversification were performed after removing each host species one at a time. X-axis shows which host species was removed from the scan.

664
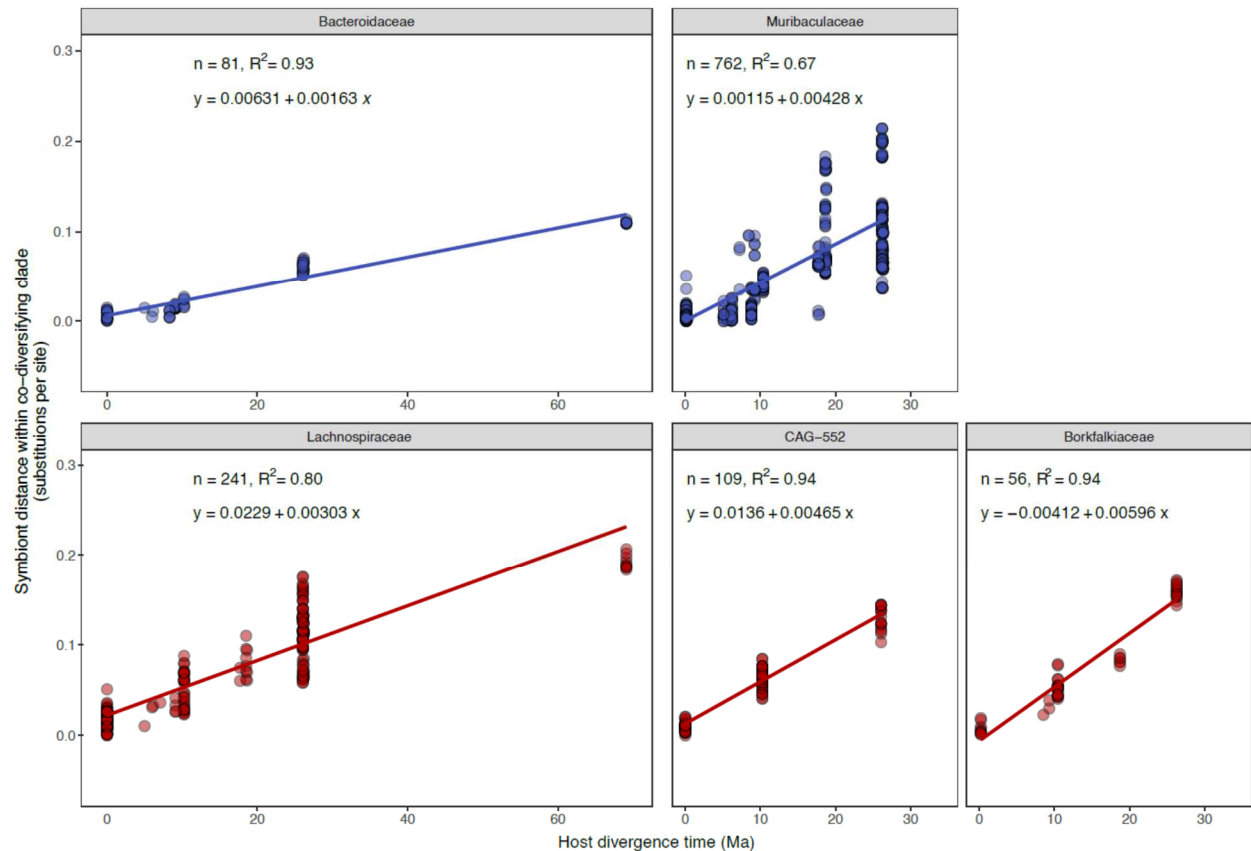
Extended Data Figure 5: Molecular clock analyses corroborate co-diversification. (A) Scatter plots show the relationship between protein sequence divergence within strongly co-diversifying symbiont clades (Mantel's r > 0.95) (y-axis) and the ages of divergence events between host clades from which they were recovered (x-axis). Lines show best-fit regressions between pairwise symbiont distances within co-diversifying clades and host divergence times. Plots are colored based on bacterial phylum as in Fig. 1, and all families containing > 2 co-diversifying clades (based on non-downsampled Hommola tests) are shown.

674
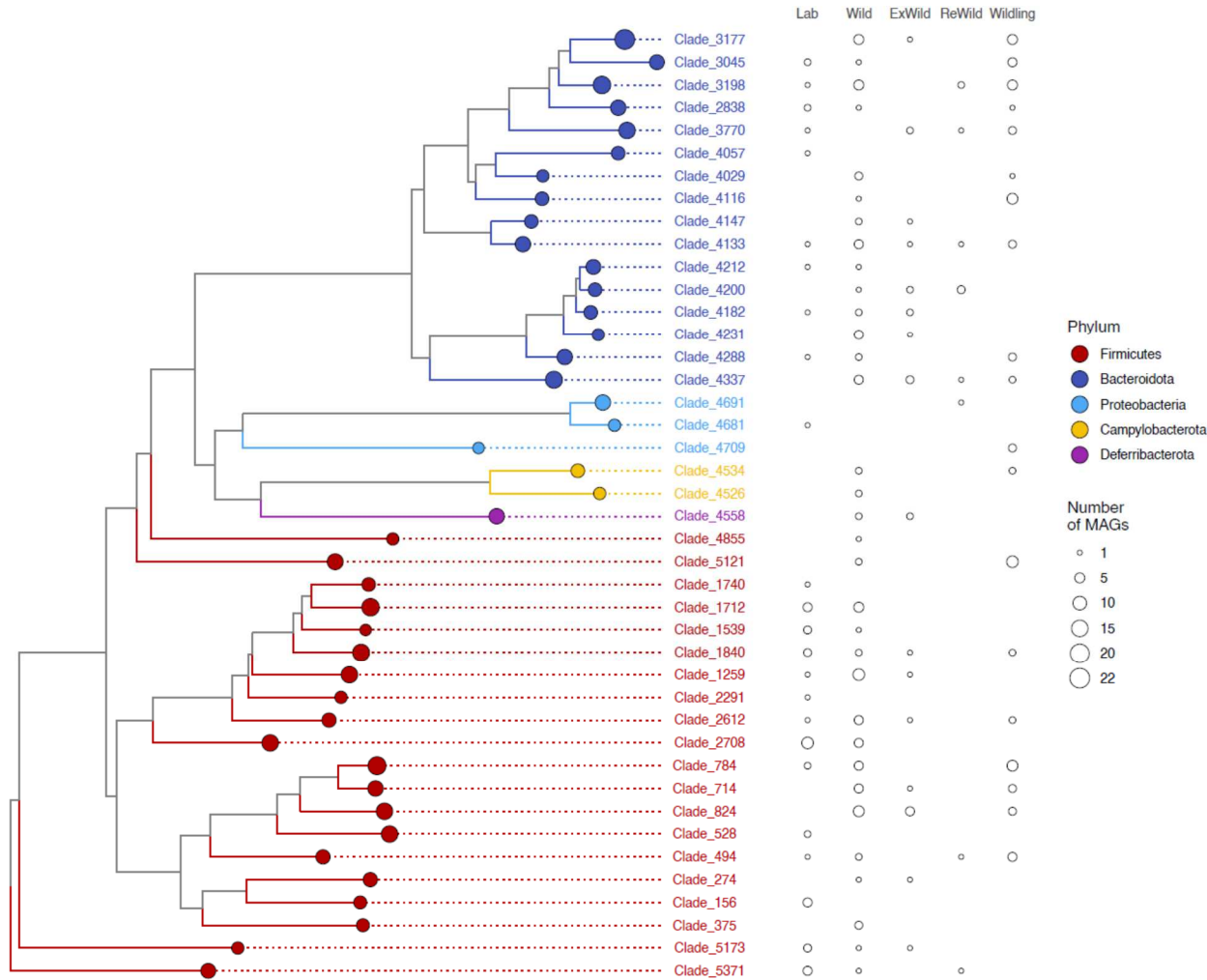
Extended Data Figure 6: Retention and extinction of ancestral, co-diversifying symbioses from laboratory house mice. Phylogeny shows relationships among all bacterial genomes belonging to co-diversifying clades shown in Fig. 1 that contain genomes from house mice, at least one other murid host, and at least one non-murid host, *i.e.*, co-diversifying clades that could be inferred to be ancestral to murids (the rodent family containing house mice). Colored circles indicate clades. Sizes of circles indicate the number of MAGs contained in the clade. Circles to the right of the phylogeny indicate the number of MAGs in each clade derived from wild mice, laboratory mice, 'rewilded' mice (*i.e.*, lab born but released and sampled outdoors), 'ex-wild' mice (wild-caught mice brought into the lab), or wildling mice (*i.e.*, laboratory genotype born to

684   wild-caught mother via embryo transfer). Rightmost two columns highlight how co-diversifying

685   clades that have been lost from laboratory mice can be regained in rewilded or wildling mice.

686
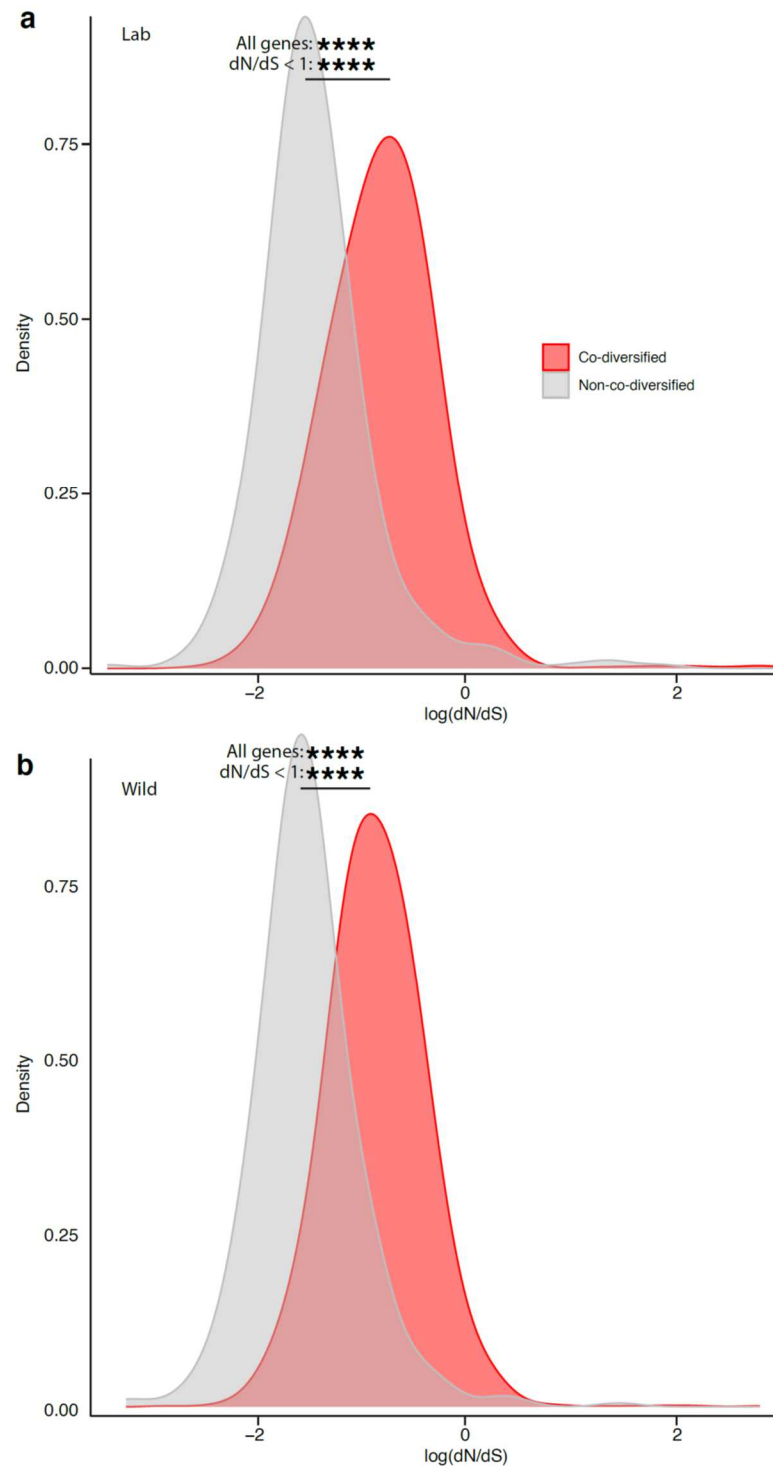
Extended Data Figure 7: Significantly elevated genome-wide genetic drift in co-diversifying relative to non-co-diversifying GM strains. a, b, Density plots show significant genome-wide elevation of dN/dS (a hallmark of genetic drift) in co-diversifying versus non-co-diversifying

691   GM clades in both laboratory house mice (**a**) and wild house mice (**b**). Significance of t-tests for

692   differences in mean are denoted by asterisks; **** *p*-value < 0.0001. Top asterisks denote

693   significance of tests considering all genes, and bottom asterisks denote significance of tests

694   considering only genes displaying dN/dS < 1 (log dN/dS < 0) in both laboratory and wild mice.

695

696
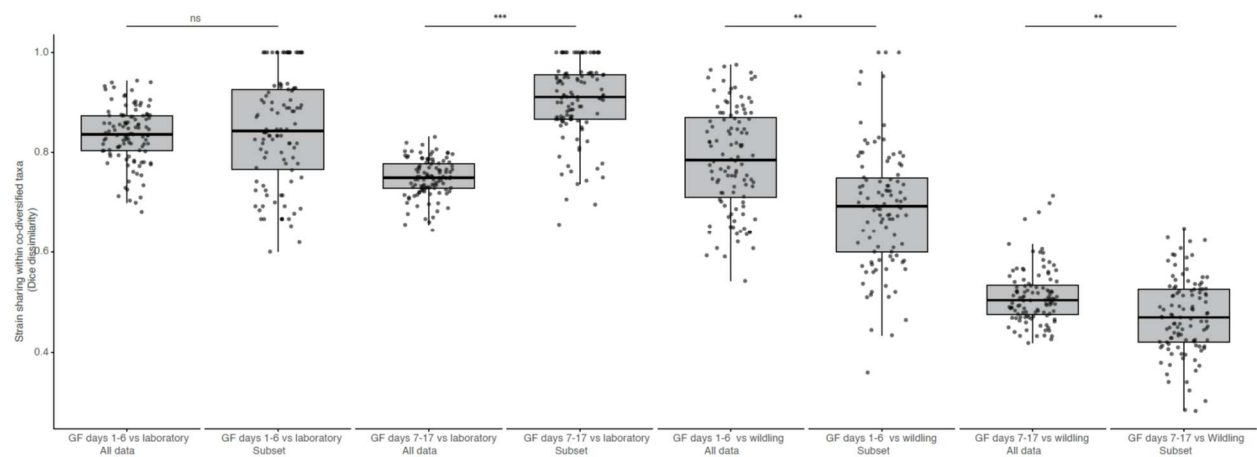
Extended Data Figure 8: Disproportionate competitive advantage of wildling ASVs from

co-diversified taxa. Boxplots show microbiota dissimilarity (Dice) based on the complete

dataset (All data) or only co-diversified ASVs retained for the analyses whose results are shown

in Fig. 4. Asterisks indicate significant differences based on permutation t-tests; *** p-value <

0.001, ** p-value < 0.01. significance testing was conducted after averaging values of

longitudinal samples from the individual mice within each group. Note the increased

dissimilarity between GF and laboratory microbiota in results based on subsetted ASVs (right

box within each facet) compared analyses based on to all ASVs (left box within each facet)

(particularly from days 7–14). Similarly, note the decreased dissimilarity between GF and

wildling microbiota in results based on subsetted ASVs compared analyses based on to all ASVs.

707

708   **Extended Data Tables**

709   **Extended Data Table 1. Metadata for *Peromyscus* samples sequenced with Nanopore.**

710   **Extended Data Table 2. Metadata for MAGs.**

711   **Extended Data Table 3. Results from co-diversification tests.** Columns labeled as 'collapsed'

712   show results of tests of clades down sampled to a single MAG per host species. Note that the last

713   25 rows do not contain symbiont trees due to string-length limits in Microsoft Excel. The

714   Newick strings for these subclades (none of which showed significant evidence of co-

715   diversification) are available at https://github.com/DanielSprockett/codiv.

716   **Extended Data Table 4. Pairwise comparisons for molecular clock estimates within co-**

717   **diversifying clades.**

718   **Extended Data Table 5. Co-diversified ($r > 0.75$) symbiont gene families under positive or**

719   **purifying selection in laboratory or wild house mice.**

720   **Extended Data Table 6. Gene families enriched in laboratory or wild house mice based on**

721   **phylogenetic ANOVA.**

722   **Extended Data Table 7. Gene families enriched in co-diversifying or non-co-diversifying**

723   **clades based on phylogenetic ANOVA.**

724   **Extended Data Table 8. Non-co-diversified ($r < 0$) symbiont gene families under positive or**

725   **purifying selection in laboratory or wild house mice.**

726   **Extended Data Table 9. Dice dissimilarities between samples from Rosshart et al.[13] based**

727   **on laboratory- and wild-specific ASVs within co-diversified taxa.**

728   **Extended Data Table 10. Read counts for laboratory- and wildling-specific ASVs from co-**

729   **diversified taxa in samples from ex-germ-free mice.**

730

731 **Supplementary Information**

732 *Nanopore metagenomic sequencing of wild-derived Peromyscus lineages*

733 We deeply sequenced the metagenomes of six species/subspecies of *Peromyscus*, including,

734 sampled at the *Peromyscus* stock center at the University of South Carolina, Columbia. Seven

735 MinION flow cells were used to sequence DNAs extracted from fecal samples, with one flow

736 cell dedicated to fecal samples from each individual host. The final *Peromyscus* dataset

737 contained 30,612,212 reads, ranging from 2,325,236 to 6,018,007 reads per sample. The average

738 per-sample read length ranged from 3,494 to 8,335 base pairs. Metadata for all *Peromyscus*

739 samples analyzed in this study are presented in Extended Data Table 1.

740

741 *Long-read assembly of bacterial genomes from Peromyscus metagenomes*

742 Assembling and binning contigs from long-read metagenomes generated by Nanopore

743 sequencing of fecal samples from the *Peromyscus* species yielded a total 504 metagenome

744 assembled genomes (MAGs) of high-quality (> 50% completeness < 5% contamination) from

745 the six host species. Bacterial diversity represented in these MAGs spanned 10 phyla, including

746 Actinobacteriota, Bacteriodota, Campylobacterota, Deferribacterota, Desulfobacterota,

747 Firmicutes, Patescibacteria, Proteobacteria, Spirochaetota, and Verrucomicrobiota. Taxonomic

748 assignments of all MAGs newly generated by this study are presented in Extended Data Table 2.

749

750 *Phylogenetic analyses of rodent MAGs and hosts*

751 Single copy bac120 core genes from each MAG were identified and aligned with GTDB-Tk, and

752 the alignment was used for phylogenetic inference with IQTree2 v2.2.0.4 with the following

753 parameters: --seed 0 -B 1000 -alrt 1000 -mset WAG,LG. *P. maniculatus sonoreinsis* was not

754   available in the timetree.org database and was therefore placed manually in the host phylogeny

755   as sister to *P. maniculatus bardii* with a divergence time of 500,000 years.

756

757   *Sensitivity analyses of co-diversification results*

758   We performed a sensitivity analysis to assess the impact of the MAGs from each individual host

759   species by conducting the Hommola co-diversification scan on each possible subset of MAGs

760   containing all MAGs except those from an individual host species. This analysis tested whether

761   the results observed in Fig. 1 depended on MAGs from any individual host species. The results

762   show that the detection of most co-diversifying clades was robust to the exclusion of MAGs

763   from any individual host species (Extended Data Figure 4). The exclusion of MAGs from *Mus*

764   *musculus domesticus* or *Rattus norvegicus*—the two host species represented by the most

765   MAGs—had the largest impact on the number of co-diversifying clades detected. However, even

766   when MAGs from one of these host species were excluded, scans identified > 100 co-

767   diversifying clades.

768

769   *Calibration of molecular clocks in the rodent gut microbiota corroborates co-diversification*

770   Given the phylogenetic evidence that symbiont lineages and host species co-diversified, the

771   known divergence dates of host species based on molecular data and fossils can be used to

772   calibrate bacterial molecular clocks[59–61], which are otherwise difficult to calibrate due to the lack

773   of a bacterial fossil record. Symbiont and host evolutionary distances within co-diversifying

774   clades were positively associated in all bacterial families (Families containing > 2 co-

775   diversifying clades are shown in Extended Data Figure 5. All data are presented in Extended

776   Data Table 4), enabling calibration of the rates of molecular evolution in diverse GM taxa. Rates

777   ranged from 0.00163 to 0.00596 substitutions per million years. These rates are within the range

778   estimated previously from codiversifying symbionts in primates[10] and timeseries data of bacterial

779   pathogens[62–64], further supporting the concurrent diversification of bacterial and rodent host

780   lineages.

781

782   *Identification of clades ancestral to Muridae*

783   We identified all co-diversifying clades that contained representatives from house mice, a non-

784   house mouse murid and at least one outgroup to the Muridae (40 non-nested, *i.e.*, independent,

785   clades). Identifying these clades allowed us to generate a set of clades ancestral to Muridae

786   independent of data from house mice, thereby enabling us to assess rates of extinction and

787   retention of these clades from either laboratory or wild house mice using a common set of

788   ancestral co-diversifying clades.

789

790   *Differentially abundant gene families between co-diversifying and non-co-diversifying clades*

791   To identify gene families enriched or depleted in co-diversifying rodent symbionts relative to

792   non-codiversifying rodent gut bacteria independent of bacterial phylogenetic history, we

793   annotated each MAG using the Kyoto Encyclopedia of Genes and Genomes (KEGG) ontogeny.

794   Next, we employed phylogenetic ANOVA[51] using the rodent gut bacterial phylogeny to identify

795   annotations over- or under-represented in co-diversifying gut bacteria ($r > 0.75$, *p*-value < 0.01)

796   relative to non-co-diversifying gut bacteria ($r < 0$). No individual annotation reached significance

797   after correction for multiple testing. These analyses provided a rank order list of gene

798   annotations significantly associated (positively or negatively) with co-diversification (Extended

799   Data Table 7).

800

801 *Tests for gain and loss of functions in genomes of laboratory–house mouse symbionts*

802 In addition to adaptive evolution of protein sequences, gut bacterial genomes can adapt to novel

803 environments through changes in gene content. Genes that benefit fitness in the new environment

804 can be gained by gene duplication or horizontal transfer and favored in bacterial populations by

805 positive selection, whereas ancestral genes that no longer provide appreciable fitness benefits can

806 be deleted by mutation (which displays a bias towards deletion in bacteria[65,66]) and lost from

807 bacterial populations by genetic drift (or, for costly genes, by negative selection). To test whether

808 the genomes of co-diversified symbionts have experienced laboratory-specific expansions or

809 contractions of specific gene families, we performed phylogenetic ANOVA for each gene family

810 in each co-diversifying symbiont clade containing MAGs from both wild and laboratory mice

811 (Supplementary Information). These analyses asked whether the genomes of multiple,

812 phylogenetically independent symbiont lineages have gained or lost—convergently or in

813 parallel—the same gene families in response to the transition from the wild into captivity. These

814 analyses provided a rank-order list of genes enriched or depleted in MAGs from laboratory house

815 mice relative to wild house mice. No gene functions were significantly enriched or depleted after

816 false-discovery correction.

817

818 *Lack of elevated genetic drift in non-co-diversifying GM clades*

819 In addition to testing for elevated genetic drift in laboratory-mouse GM strains in co-diversifying

820 clades (r > 0.75), we also tested for elevated genetic drift in laboratory-mouse GM strains in non-

821 co-diversifying clades (r < 0) of similar phylogenetic depth to co-diversifying clades (*i.e.*, clades

822 of congeneric MAGs in the distal 1/4th of bacterial phylogeny). These analyses did not support a

823 significantly increased genetic drift, as measured by genome-wide elevation of dN/dS, in non-

824   codiversifying clades (paired t-test p-values = 0.0944 for tests based on genes under purifying

825   selection, *i.e.*, genes for which dN/dS was < 1 in both wild-mouse and lab-mouse GM strains),

826   contrasting the results observed for co-diversifying clades (Extended Data Table 8). Tests on

827   individual non-co-diversifying clades also failed to strongly support increased genome-wide

828   dN/dS in non-co-diversifying laboratory-mouse GM strains (paired t-test FDR-corrected p-

829   values > 0.01 for all clades, and > 0.1 for all but 1 clade). A single clade (node 5493: an

830   unclassified genus, CAG-1435, in the order Christensenellales) showed a marginally significant

831   elevation in dN/dS in laboratory-mouse GM strains relative to WGM strains (paired t-test FDR-

832   corrected p-value = 0.0241), and when all genes were tested, a marginally significant increase in

833   dN/dS in the laboratory-mouse GM strains was observed (paired t-test p-values = 0.04065). This

834   latter difference can be attributed to genes showing evidence of positive selection (dN/dS > 1) in

835   laboratory-mouse GM strains but purifying selection (dN/dS < 1) in WGM strains, rather than

836   increased genetic drift. Cumulatively, these results indicate that the significant elevation of

837   genome-wide dN/dS (indicative of reduced Ne and increased genetic drift) in laboratory house

838   mice observed for co-diversified GM strains was not apparent for non-co-diversified GM strains.

839

840   *Elevated genetic drift in co-diversifying relative to non-co-diversifying clades in both laboratory*

841   *and wild house mice.*

842   Significant evidence of elevated genetic drift in laboratory GM strains was detected in co-

843   diversifying clades but not non-co-diversifying clades (Tables S5, S8), suggesting that co-

844   diversifying clades may be particularly predisposed to elevated genetic drift. Previous studies of

845   insect endosymbionts have shown that bottlenecks during transmission of host-restricted

846   symbionts can promote genetic drift[12,13], but the extent to which host-restriction of GM

847   symbionts in mammals promotes genetic drift has not been explored. To address this idea, we

848   tested whether co-diversifying clades displayed stronger evidence of genetic drift than non-co-

849   diversifying clades regardless of environment (laboratory or wild). We compared the

850   distributions of per-gene log(dN/dS) values between co-diversified and non-co-diversified clades

851   in both the laboratory and the wild. Results indicated significant elevation of genetic drift, as

852   indicated by elevated genome-wide dN/dS, in co-diversified relative to non-co-diversified GM

853   clades (Extended Data Figure 7) in both the laboratory (Extended Data Figure 7A) and the wild

854   (Extended Data Figure 7B). These findings suggest that the host restriction of co-diversified

855   clades predisposes these lineages to stronger genetic drift, which can be further enhanced by

856   transitions from the wild to the laboratory environment (Fig. 3).

857

858   *Removal of co-diversifying ASVs reduces signal of competitive advantage for wildling*

859   *microbiota*

860   To test whether ASVs of wildling or laboratory origin within co-diversifying taxa displayed a

861   disproportionately strong competitive differential (compared to all ASVs), as suggested by

862   Extended Data Figure 8, we compared results of beta-diversity analyses based on the complete

863   dataset with those based on the complete dataset minus the ASVs used in analyses whose results

864   are shown in Fig. 4. This comparison allowed us to test whether the removal of these ASVs

865   belonging to co-diversifying taxa reduced the measured competitive differential between

866   wildling and laboratory microbiota, as expected if co-diversifying laboratory GM strains have

867   acquired increased genetic load. Indeed, removing these ASVs led to weaker signal of

868   competitive advantage for wildling microbiota. On average, when all ASVs were included, the

869   Dice beta-diversity differential between GF day 7–14 versus laboratory microbiota and GF 7–14

870   versus wildling microbiota was 0.237 (favoring wildling microbiota), whereas when only the

871   subsetted ASVs (as defined in Fig. 3 and Extended Data Figure 8) were included this differential

872   reduced to 0.22 (the difference in differential of only ~0.01, given that the subsetted ASVs

873   constituted 105 of 2640 total ASVs. These findings indicate that laboratory-derived GM strains

874   belonging to co-diversifying taxa displayed disproportionately stronger evidence for reduced

875   fitness in these experiments than did other laboratory-derived GM strains, mirroring results

876   presented in Extended Data Figure 8. These findings further support increased genetic load in

877   laboratory-derived GM strains in co-diversifying taxa.

878   **Supplemental References**

879   59. Moran, N. A., Munson, M. A., Baumann, P. & Ishikawa, H. A molecular clock in
880   endosymbiotic bacteria is calibrated using the insect hosts. *Proc. R. Soc. Lond. Ser. B: Biol. Sci.*
881   **253**, 167–171 (1993).

882   60. Ochman, H., Elwyn, S. & Moran, N. A. Calibrating bacterial evolution. *Proc. Natl. Acad.*
883   *Sci.* **96**, 12638–12643 (1999).

884   61. Ochman, H. & Wilson, A. C. Evolution in bacteria: Evidence for a universal substitution rate
885   in cellular genomes. *J. Mol. Evol.* **26**, 74–86 (1987).

886   62. Duchêne, S. *et al.* Genome-scale rates of evolutionary change in bacteria. *Microb. Genom.* **2**,
887   e000094 (2016).

888   63. Menardo, F., Duchêne, S., Brites, D. & Gagneux, S. The molecular clock of *Mycobacterium*
889   *tuberculosis. PLoS Pathog.* **15**, e1008067 (2019).

890   64. Rascovan, N. *et al.* Emergence and spread of basal lineages of *Yersinia pestis* during the
891   Neolithic decline. *Cell* **176**, 295-305.e10 (2019).

892   65. Sela, I., Wolf, Y. I. & Koonin, E. V. Theory of prokaryotic genome evolution. *Proc. Natl.*
893   *Acad. Sci.* **113**, 11399–11407 (2016).

894   66. Kuo, C.-H. & Ochman, H. Deletional bias across the three domains of life. *Genome Biol.*
895   *Evol.* **1**, 145–152 (2009).

896